# Peer Review File

**Manuscript Title:** Long-Range Ordered Porous Carbons Produced from C60

## Editorial Notes:

**Redactions – unpublished data**

Parts of this Peer Review File have been redacted as indicated to maintain the confidentiality of unpublished data.

## Reviewer Comments & Author Rebuttals

**Reviewer Reports on the Initial Version:**

Referees' comments:

Referee #1 (Remarks to the Author):

The authors describe a synthesis and detailed characterisation of a long range ordered open cage structure of C60. The synthesis is driven by a mixing of pristine C60 with LiN3 accompanied with a charge transfer from Li to the C60 structure.

The study is interesting but before a decision can be made a significant revision needs to be made, where to start with the following points need to be considered.

The role of the polymerisation and the breaking of the cages is clearly related to the charge transfer from Li to C60. It is therefore highly odd that the authors do not better connect their results to previously published literature in the field of alkali metal doped C60, in specific the papers published on Li-doped C60. The synthesis conditions used in the current study, that is by Li3N is related to the conditions used by Ricco, et al, [Ricco, PHYSICAL REVIEW B, Volume, 72, 15, Article Number, 155437] who uses LiN3 and to the work by Wagberg et al who performs the synthesis by using pure Li [Wagberg et al, Journal of Physics and Chemistry of Solids 65 (2004) 317–320], as well as to other work in this area. The authors need to clearly relate their work to previous work in this field, as well as referring to polymerisation by doping, a very well-known and well-studied field for several of the AxC60-phases (A = Li, Na, K).
Given the conditions, the mixture 500 mg of C60 (molar weight = 720 g/mol) and 100 mg of Li3N (20 g/mol) gives 1.44 mole of C60 and 15 mole of Li, which gives roughly 10 Li per C60 molecule. The stoichiometry needs to be better addressed. Since the conditions are close to the structure Li12C60 that is reported as a sort of super cluster structure [Cristofolini, et al, Lithium diffusion and C60 dynamics by quasielastic and inelastic neutron scattering in Li12C60 fulleride, Physical Review B, 61, 3404, 2000] which is reported to transform to a fcc phase at 550 K, it is likely that the synthesis at higher temperatures will go through a doping and polymerisation which likely starts by a gradual polymerisation by well-known 2+2 cycloaddition and perhaps even a single bond polymerisation in the other direction. How that structure develops due to electron transfer changes when washing away the Li is interesting, but not well-addressed.
1) The authors need to describe how the structure changes at different ratios between Li and C60.

2) Model the position of the Li at the synthesis conditions.
3) Give better data on the structure before the washing procedure
4) Explain why the washing is made even more times for the higher reaction temperatures?
5) When the annealing temperature was reduced to about 480 C the authors obtain a C60 polymer after washing. It is not clear why this phase is formed, and the reaction conditions during the washing procedure need to be better investigated. A linear orthorhombic polymer obtained by charge transfer is normally obtained at low charge transfer (for example the A1C60-phases). This could be explained by either a steric hindrance at 480 C which somehow leads to a polymerisation that cannot evolve further or due to Li-remnants that develop to a doped polymer phase during the washing procedure. The authors should look into this.
6) The in-situ MAS-NMR should be presented so that the spinning side bands can be observed, since they would directly reveal when the C60 becomes static. From figure S14 b this seems to occur around roughly 260 C (530 K) which would correspond perfectly with the conditions used to for the alkali-doped polymer phases (Li4C60, Na4C60…).
7) I do not agree that the Raman spectra of LOPC at all matches the contour of the simulated spectrum. It is also unclear why the 1449-peak in the simulated spectra would be related to the pentagonal pinch mode. The 1455 peak in figure 1 d is also not visible, and it is therefore difficult to follow discussions on this peak.
8) The MAS-NMR reveal a sp3 peak at 76 ppm. The intensity of this peak should be related to the sp2 carbon (143 ppm) in order to estimate the covalent sp3-bonding in the structure.
9) It would be helpful to show MAS-NMR also before washing to reveal the effect of charge transfer (which should go away after removing the Li).
10) The MAS-NMR should be compared to the 13-C NMR obtained by [Ricco, PHYSICAL REVIEW B, Volume, 72, 15, Article Number, 1554379]. The different components in the 143-ppm band should represent sp2 carbon-atoms with different chemical environement. The authors need to better correlate these to the different carbons in their structural models. It is unclear why the 14.2-peak has higher FWHM than the rest. This might indicate that a fifth peak should be added. It might be possible to correlate the MAS-NMR to the neutron scattering analysis.
11) Li-7 MAS-NMR, as performed in [Journal of Physics and Chemistry of Solids 67 (2006) 1091–1094] before washing would be able to reveal the location of the Li-atoms, and thus also explain better the mechanism of the polymer/cage breaking formation.
12) The resistance measurements are not well-described. First of all the resistance to high extent will be dominated by grain boundaries. What are the sizes of the “crystalline domains” as determined from XRD and FFT?

In total there are still a number of issues that need to be clarified before a decision can be made on the suitability of the manuscript to be published.

Referee #2 (Remarks to the Author):

In our traditional knowledge of crystallography, solid-state materials are categorized by their structures into three types, e.g., crystalline (having periodic translation symmetry), amorphous (no

periodic and orientational symmetry), and quasi-crystalline (having orientational but not periodic translation symmetry) phases. Ten years ago, Wang et al. (Science 2012, 337, 825) first discovered a hexagonal close-packed long range ordered amorphous carbon clusters through the direct high pressure transformation of C60 using a diamond anvil cell. The discovery changes our long term understanding of the inherent disorder (amorphous building block) that cannot be present in a crystal (Science 2012, 337, 812). Unfortunately, the quantity of the sample obtained under high pressure is very limited, usually in a scale of milligrams or less, and therefore hinders the further explorations on their properties and potential applications. The present paper reports the first long range ordered porous carbon (LOPC) in a face centered cubic lattice, which can readily be produced using a chemical protocol in gram-scale at room pressure and moderate temperature. This tremendous step opens new opportunities for use of the products in new ways, and also for doing further chemistry on the products to generate other downstream products that might have interesting properties and functionalities.

The gram-scale LOPC is prepared from C60 powder with electron transfer from α-Li3N at 550°C and ambient pressure. It was clearly determined that LOPC consists of connected 'broken' C60 cages that however maintain long-range periodicity using a variety of characterizations including X-ray diffraction, Raman spectroscopy, magic angle spinning solid state nuclear magnetic resonance spectroscopy, aberration-corrected transmission electron microscopy, and neutron scattering. The simulations based on neural network show that LOPC is a metastable structure in the evolution from fullerene type to graphene type carbons, providing an understanding of the transformation from C60 to LOPC. In my opinion, the result presented in the paper is convincing and of great importance to the fields of crystallography and materials science. It deserves to be published in Nature if the following issues/comments could be well addressed.

1. About XRD:
It is known from the structure of long range ordered carbon clusters that the atomic structure and orientation of the crushed C60 clusters are not identical to each other. So, the x-ray diffraction of the LOPC should have two contributions: sharp diffraction peaks from fcc lattice and diffused hump from local disordering. This coexistence is clearly seen in the XRD date (figure 1b and 1c) and is crucial for the conclusion made in the paper.
In the simulated XRD, there are two obvious extra peaks (at ~12.5 and ~24 degree) as compared to the measured one in figure 1b. How was the simulation carried out, and what is the structural model used in the simulation? I guess the identical carbon clusters are used in the simulation, in such a case the two extra diffraction peaks will appear because of large structure factor. In fact, the atomic structure of crushed C60 should be disorder and the orientation must be somehow random. The authors need to point it out and add a short discussion in revision.

2. About Raman spectrum
Pristine C60 has ten Raman modes including 8 Hg and 2 Ag. However, there several unknown peaks exist in the Raman spectrum shown in figure 1a, which should be clarified. The Raman peaks of the C60 polymer should be indexed as well.

3. Low-pressure adsorption/desorption
Many experimental details are missing in either the manuscript or supplementary. For example, the

caption of figure 1f says “low-pressure Ar (87.3K) ...”, but with no description. Is the absorption/desorption measurement carried out at low temperature? 87.3 K is almost the liquidizing temperature of Ar.

4. The thermal stability:
More characterizations of TGA and mass spectrum are encouraged to be added. Mass spectrum and TGA studies on the LOPC could provide solid evidence of its characteristics. They will put more weights on the reliability of the conclusion made.

5. The application of battery:
As seen from figure S19, LOPC does not show obvious superior advantage in the application as an anode for lithium and sodium ion batteries. I would like to suggest the author to remove the last sentence of the article : “ As an example, LOPC has shown potential applications ...”, as the discovery of the first fcc LOPC and the gram-scale yield are already importance enough for its publication in a prestigious journal like Nature.

6. Writing and organization of the paper:
The results in the paper are important and convincing. However, it is not a well written and organized paper. I think it must be easy for the authors especially the native speaker in the list to help this out.

7. Format of references:
It is realized that format of the cited references are incorrect. It should be taken care of according to the requirement of the journal Nature.

Referee #3 (Remarks to the Author):

In the Manuscript titled: “Long-Range Ordered Porous Carbon from C60” Pan F. and collaborators claim the discovery of a new type of carbon. The authors report a simple and scalable method involving mixing α-LiN3 with C60 and heating at 550 °C followed by some purification steps. Currently, the synthesis method is capable of producing large batches around one gram per batch and can be easily scaled to kilograms of more.
The building blocks for this new material are damaged C60 cages interconnected by sp2 carbon-carbon links. Some of the properties of the material are compared with pristine C60 powders and C60 polymer crystal which are closely related forms of carbon. The authors perform an extensive characterization of the crystalline structure of the material by several techniques including X-Ray diffraction, aberration corrected transmission electron microscopy and Raman spectroscopy and confirm that the broken C60 cages exhibits a long-range arrangement. In this study the authors find that this is a metastable form of carbon between C60 and graphene.
A characterization of the electrical conductivity of the material to results on a value of 1.17x10-2 S cm-1, representing an enhancement of several orders of magnitude when compared with pristine C60 or C60 polymer crystal. Low temperature electrical characterization revealed a possible

transition from semiconductor to metallic properties as LOPC is synthesized at higher temperatures. The manuscript shows a novel form of synthetic carbon and a very detailed characterization of the crystalline structure, as well as computational exploration of its electronic structure. However, the manuscript is presented in a form that makes it appealing mostly to the carbon science and the materials science communities, but not for a broader audience; the manuscript lacks of an outstanding property, a specific application or the explanation of the extreme importance of this discovery, because of that, I don't believe its suitable for publication in nature

Referee #1 (Remarks to the Author):

The authors describe a synthesis and detailed characterization of a long range ordered open cage structure of $C_{60}$. The synthesis is driven by a mixing of pristine $C_{60}$ with $LiN_3$ accompanied with a charge transfer from Li to the $C_{60}$ structure.

The study is interesting but before a decision can be made a significant revision needs to be made, where to start with the following points need to be considered.

**Response**: Thank you for reviewing our paper.

The role of the polymerization and the breaking of the cages is clearly related to the charge transfer from Li to $C_{60}$. It is therefore highly odd that the authors do not better connect their results to previously published literature in the field of alkali metal doped $C_{60}$, in specific the papers published on Li-doped $C_{60}$. The synthesis conditions used in the current study, that is by $Li_3N$ is related to the conditions used by Ricco, et al, [Ricco, PHYSICAL REVIEW B, Volume, 72, 15, Article Number, 155437] who uses $LiN_3$ and to the work by Wagberg et al who performs the synthesis by using pure Li [Wagberg et al, Journal of Physics and Chemistry of Solids 65 (2004) 317–320], as well as to other work in this area. The authors need to clearly relate their work to previous work in this field, as well as referring to polymerization by doping, a very well-known and well-studied field for several of the $A_xC_{60}$-phases (A = Li, Na, K).
Given the conditions, the mixture 500 mg of $C_{60}$ (molar weight = 720 g/mol) and 100 mg of $Li_3N$ (20 g/mol) gives 1.44 mole of $C_{60}$ and 15 mole of Li, which gives roughly 10 Li per $C_{60}$ molecule. The stoichiometry needs to be better addressed. Since the conditions are close to the structure $Li_{12}C_{60}$ that is reported as a sort of super cluster structure [Cristofolini, et al, Lithium diffusion and $C_{60}$ dynamics by quasielastic and inelastic neutron scattering in $Li_{12}C_{60}$ fulleride, Physical Review B, 61, 3404, 2000] which is reported to transform to a fcc phase at 550 K, it is likely that the synthesis at higher temperatures will go through a doping and polymerisation which likely starts by a gradual polymerisation by well-known 2+2 cycloaddition and perhaps even a single bond polymerisation in the other direction. How that structure develops due to electron transfer changes when washing away the Li is interesting, but not well-addressed.

**Response**: Please note that we have used $Li_3N$ (35 g/mol) instead of $LiN_3$ (49 g/mol) in our work (that is, our compound is different). The use of $LiN_3$ was reported in *J. Am. Chem. Soc. 2004, 126, 15032* (abbreviated as 'JACS 2004 paper' in the following discussion) and in *Phys. Rev. B 2005, 72, 155437*. The corresponding author of the 'JACS 2004 paper' has, by email to us, confirmed that they referred to lithium azide ($LiN_3$) as "$Li_3N$" in their paper by mistake, as shown in Fig. R1 **[REDACTED]**. A study has shown that lithium azide ($LiN_3$) would decompose into lithium nitride ($Li_3N$) at 260 °C instead of metallic li thium (*Energy Environ. Sci., 2011, 4, 3625-3631*), following the reaction $3LiN_3 \rightarrow Li_3N + 4N_2$. We believe that, compared to lithium azide ($LiN_3$), lithium nitride ($Li_3N$) would have a more direct impact on the formation of carbons in the preparation, *e.g.*, by releasing Li at high temperatures as discussed below.

**[REDACTED]**

In our previous study (*Nano Lett. 2021, 21, 5648-5654*), we have shown that lithium nitride ($Li_3N$) shows a strong "ability" for electron donation to graphite. To further evaluate the interaction between $\alpha$-$Li_3N$ and $C_{60}$, we performed additional ab-initio molecular dynamics (AIMD) simulations and found that $\alpha$-$Li_3N$ would decompose in the presence of $C_{60}$ at high temperatures, as shown in Fig. R2 below. This may connect the formation of $C_{60}$ polymer crystal and LOPC in the current work with previous studies based on Li-doped $C_{60}$(s), although in previous reports several weeks of Li deposition was needed to achieve the intercalation, ***e.g.***, forming $Li_4C_{60}$ (*J. Phys. Chem. Solids 2004, 65, 317-320; J. Phys. Chem. Solids 2006, 67, 1091-1094*). In the revised manuscript we have added more discussion related to reports on alkali metal-doped $C_{60}$(s), and specifically to studies of Li-doped $C_{60}$(s).

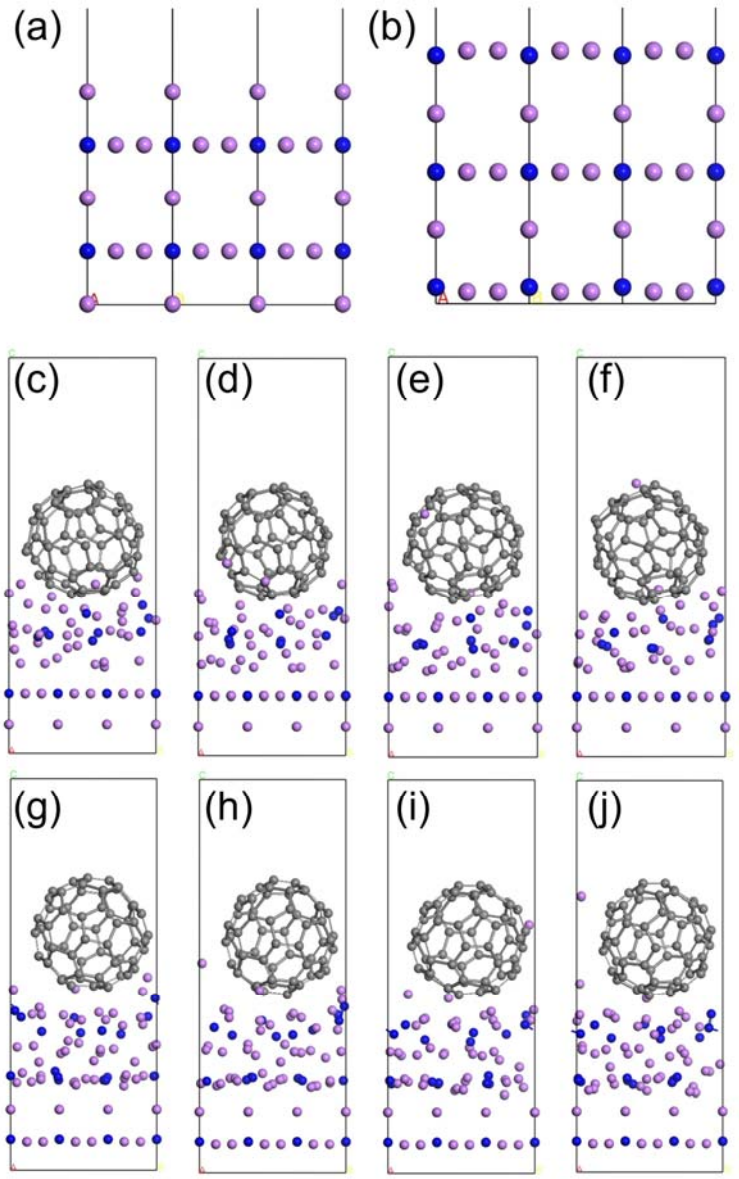


Fig. R2. (a) Li and (b) LiN exposed surface of $\alpha$-$Li_3N$ crystal along <001> direction; (c-f) show a Li atom diffusion at 1500 K on a $C_{60}$ surface on an exposed Li surface; (g-j) show a Li atom diffusion on a $C_{60}$ surface at less than 1000 K on an exposed LiN surface. A 3×3×1 supercell of $\alpha$-$Li_3N$ (001) surface is considered so as to match the lattice of a $C_{60}$ molecular crystal in the <111> direction. Two atomic layers at the bottom of $\alpha$-$Li_3N$ are fixed during the AIMD simulation.

1) The authors need to describe how the structure changes at different ratios between Li and $C_{60}$.

**Response**: We have prepared new samples by annealing 500 mg $C_{60}$ with different amounts of $Li_3N$, *e.g.*, 50, 75, 100, 125, 150, or 400 mg at various temperatures between 440 and 600 °C; the XRD patterns are shown in Fig. R3. A phase diagram based on the structures from all XRD data is shown in Fig. R4. By comparing the features of XRD patterns with those of a $C_{60}$ polymer crystal and LOPCs in the manuscript, we see that the formation of a $C_{60}$ polymer crystal depends on both temperature and $Li_3N/C_{60}$ ratio, for the same annealing time of 5 h. More $Li_3N$ is needed to obtain the same carbons at the lower temperatures; the formation of LOPCs occurs in a quite narrow range of conditions, *e. g.*, from 540 to 560 °C for a $C_{60}/Li_3N$ ratio of 500 mg/100 mg and 5h annealing (refer to Fig. 1c in the manuscript). The phase diagram and more XRD data have been added in the revised Supplementary Information to better illustrate the preparation conditions.

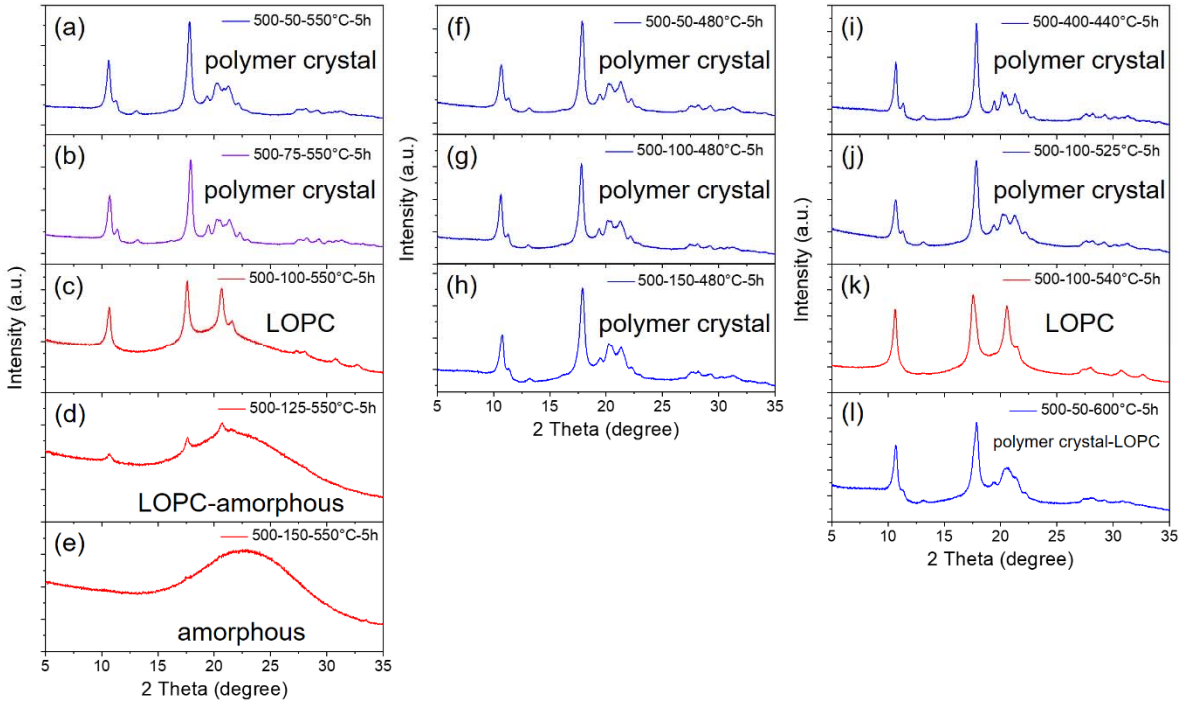


Fig. R3. Cu $K_\alpha$ ($\lambda$ = 0.15418 nm) XRD patterns of samples (after washing with toluene and deionized water) prepared (a-e) by annealing 500 mg $C_{60}$ with 50/75/100/125/150 mg $Li_3N$ at 550 °C; (f-h) by annealing 500 mg $C_{60}$ with 50/100/150 mg $Li_3N$ at 480 °C; by annealing 500 mg $C_{60}$ (i) with 400 mg $Li_3N$ at 440 °C, (j, k) with 100 mg $Li_3N$ at (j) 525 °C and (k) 540 °C, or (l) with 50 mg $Li_3N$ at 600 °C.

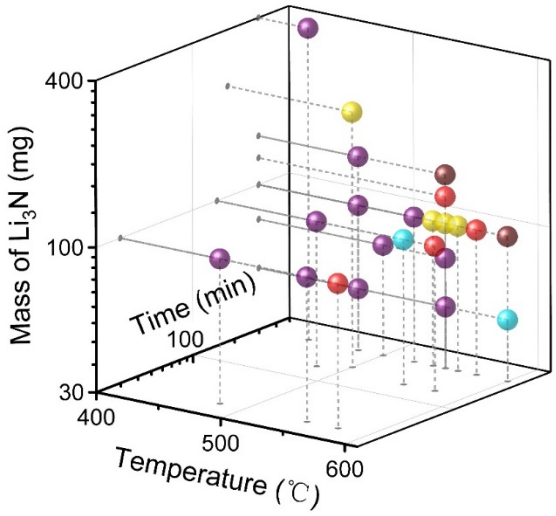


Fig. R4. Products depending on the preparation conditions for $C_{60}$ polymer crystal (purple), polymer crystal-LOPC mixture (blue), LOPC (yellow), LOPC-amorphous mixture (red) and amorphous (brown). The 'sorting' of structures is based on the powder XRD spectra of all of these samples.

2) Model the position of the Li at the synthesis conditions.

**Response**: Because $\alpha$-$Li_3N$ was found to decompose in the presence of $C_{60}$ during annealing, we have also performed additional AIMD simulations to model the intercalation of Li into a $C_{60}$ molecular crystal. The temperature was controlled from 300 to 5000 K during simulations and the total simulation time was 100 ps with a time step of 1 fs, corresponding to a heating rate of 47 K $ps^{-1}$. Three distinct occupation sites were considered, namely the octahedral site (**O** site), the tetrahedral site (**T** site) and a planar triangle center site (**T'** site), as shown in Fig. R5. Note that the **T'** site is nearly planar, and would be with a small out-of-plane displacement of ~ 0.2 Å, based on the DFT optimization. Three models were considered: (i) $LiC_{120}$ model with single Li atom intercalation at the **O** site, which is the largest space in fcc $C_{60}$; (ii) $Li_6C_{120}$ model with Li atoms initially occupying all **O** and **T** sites; and (iii) $Li_{16}C_{120}$ model with Li atoms initially occupying all **T'** sites.

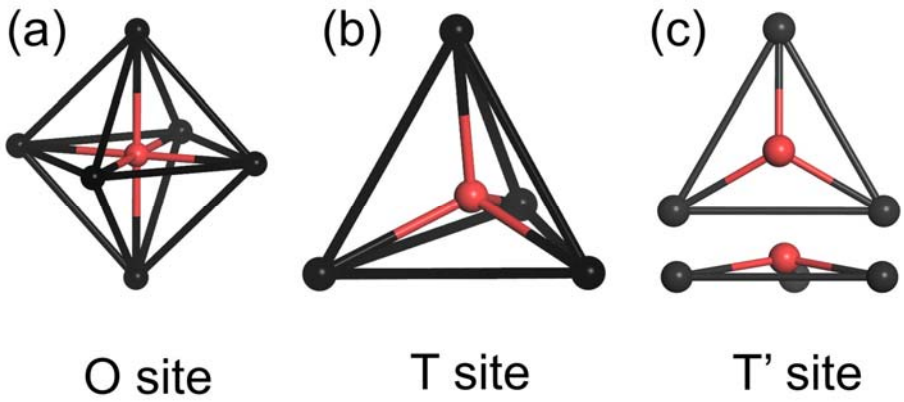


Fig. R5. Illustration of (a) **O**, (b) **T** and (c) **T'** sites. The black balls denote the positions of $C_{60}$ and the red balls denote Li sites.

The simulation results are shown in Fig. R6, in which (a), (c), and (e) show the time-dependent change of temperature and potential energy; (b), (d), and (f) show the changes in the sites occupied by the Li atoms. From the simulations we can see that the $C_{60}$ cages in the $LiC_{120}$ model remain unchanged through the simulation, as shown in the inset of Figure R6 (a), but the cages collapse at ~ 4200 K in $Li_6C_{120}$ and at ~ 4000 K in $Li_{16}C_{120}$, resulting in the connection between broken cages and the formation of more amorphous structures, as shown in the insets of Figs. R6 (c) and R6 (e).

For the $LiC_{120}$ model, we find that Li is first trapped in the initial O site, then hops out at ~ 6.9 ps (~ 600 K) to the **T** and **T'** sites. After that, Li diffuses in the $C_{60}$ crystal with a greater possibility of occupying the **T'** site. For the $Li_6C_{120}$ model, we find that Li atoms diffuse into **T'** sites at the very beginning of the simulation and the possibility of occupying the **T'** site is larger than that of occupying the **O** and **T** sites. For the $Li_{16}C_{120}$ model, Li atoms initially occupy the **T'** sites, then diffuse into **T** sites at ~6.1 ps (~ 550K) and into **O** sites at ~13.1ps (~ 950 K). Thus, from simulations we can suggest that the breaking of $C_{60}$ cages is accelerated by the introduction of more Li and higher annealing temperatures.

More discussion has been added to illustrate the role of $Li_3N$/Li on the formation of LOPC in the revised manuscript.

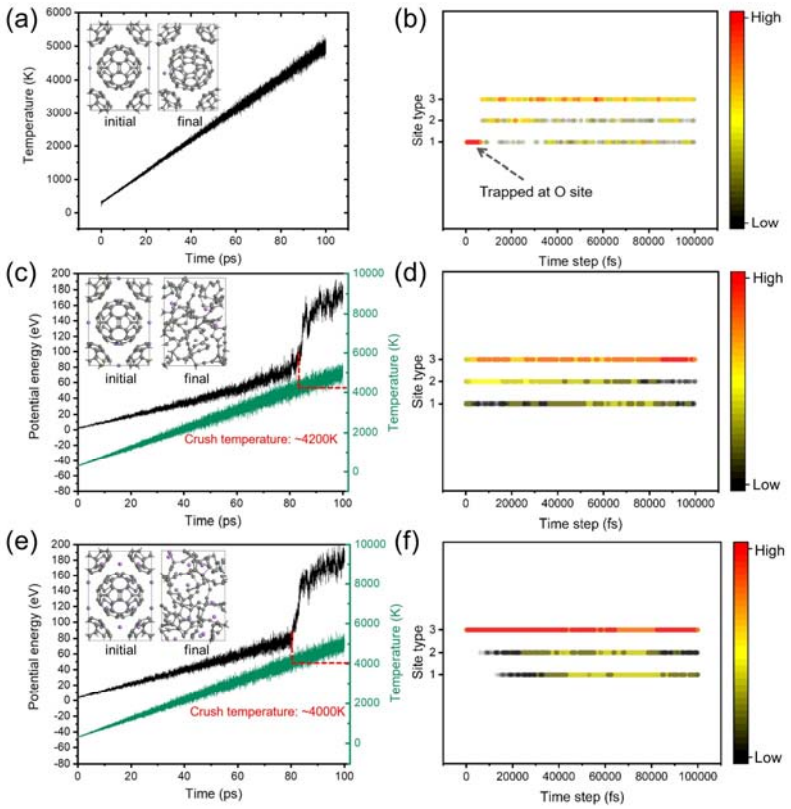


Fig. R6. Change of temperature and potential energy over time for (a) $LiC_{120}$, (c) $Li_6C_{120}$ and (e) $Li_{16}C_{120}$ models. The insets show the initial and final structures during AIMD simulations. The grey balls denote C atoms and purple balls denote Li atoms. Time-dependent occupation of Li atoms in **O** sites (type 1), **T** sites (type 2) and **T'** sites (type 3) for (b) $LiC_{120}$, (d) $Li_6C_{120}$ and (f) $Li_{16}C_{120}$ models. The color bar shows the density of the points, indicating the possibility of their being occupied by Li atoms when the number of points is sufficiently large, *e.g.*, 20000 points for Fig. R5b, 120000 points for Fig. R5d and 320000 points for Fig. R5f. The occupied site is defined as the site (type 1, 2, or 3) closest to the Li atom.

3) Give better data on the structure before the washing procedure.

**Response**: To evaluate the structural evolution of carbon and Li/$Li_3N$ additional XRD has been carried out on samples after the annealing (cooling but without any washing) or samples after washing by toluene only (drying but without washing with water), as shown in Fig. R7. By comparing the spectra, we conclude that a $C_{60}$ polymer crystal or LOPC is formed before washing, as the disappearing diffraction peaks after washing with toluene are only ascribed to fcc-$C_{60}$ or $Li_4C_{60}$, and the diffraction peaks of a $C_{60}$ polymer crystal or LOPC remain nearly unchanged after washing. Those peaks assigned to $Li_2CO_3$ disappear after subsequent washing by deionized water. Data have been added in the revised Supplementary Information to illustrate the influence of washing.

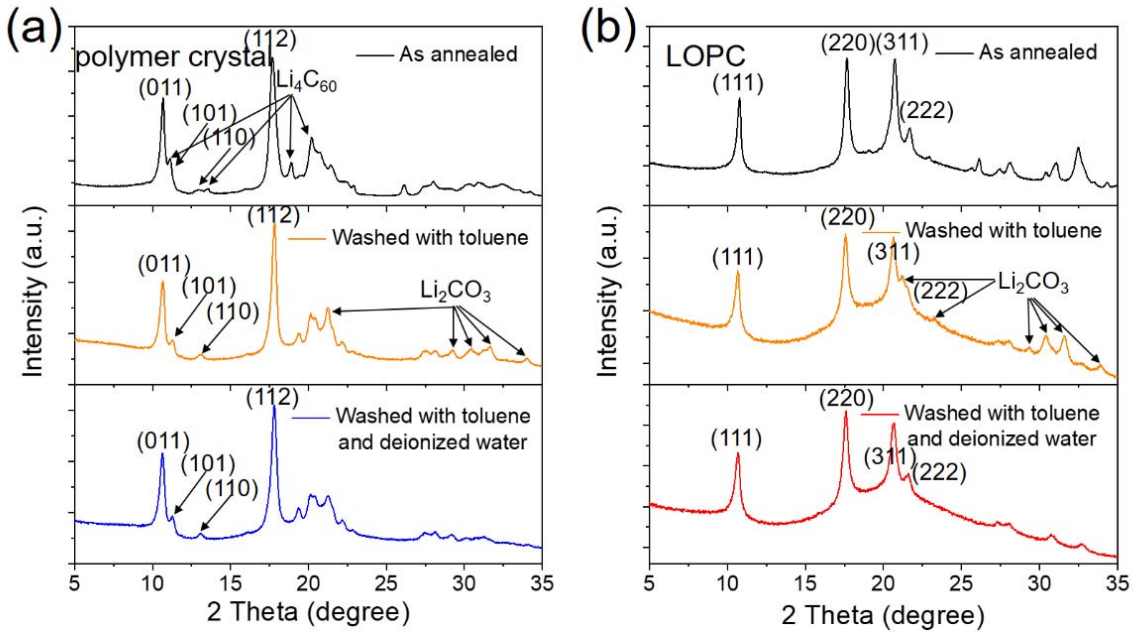


Fig. R7. Cu $K_\alpha$ ($\lambda$ = 0.15418 nm) XRD patterns of samples before and after washing, made by annealing 500 mg $C_{60}$ with 100 mg $Li_3N$ (a) at 480 °C for the polymer crystal and (b) at 550 °C for LOPC.

4) Explain why the washing is made even more times for the higher reaction temperatures?

**Response**: To figure out the location (or penetration depth) of Li (atoms or salts) in the carbon after annealing, additional $^7$Li MAS-NMR has been carried out before and after washing and the spectra are shown in Fig. R8. From the spectra we can observe the sharp peak at ~ 0 ppm in both a $C_{60}$ polymer crystal and LOPC, originating from residual diamagnetic Li salts such as $Li_2CO_3$ in these samples (please see Figure R6, and also refer to *Chem. Mater. 2019, 31, 2545~2554*). Compared with the $C_{60}$ polymer crystal, a wider peak centered at ~ -3 ppm has been observed from LOPC, which may be explained by Li ions coupled to the defects in LOPC yet with a complicated chemical environment. It is more difficult to remove such Li, because the adsorption of Li at the defects is stronger than on the plane(*Carbon, 2014, 80, 305-310*), thus more washing is needed to purify the LOPC samples. As a reference, an NMR peak of Li at -10.5 ppm was observed from Li

endohedral $C_{60}$ (*Nat. Chem. 2010, 2, 678-683*). $^{7}$Li MAS-NMR data have been added in the revised Supplementary Information.

It is worth noting that, although we have seen a clear $^{7}$Li MAS-NMR signal due to the high natural abundance (92.4%) of $^{7}$Li (spin-3/2), high gyromagnetic ratio ($\gamma(^{7}Li)/\gamma(^{1}H)$ = 0.39) and small quadrupolar couplings (*J. Am. Chem. Soc. 2020, 142, 17447-17456*), the content of Li is essentially lower than 1% in both a $C_{60}$ polymer crystal and LOPC, as indicated by the very low residual mass ($Li_2O$ or $Li_2CO_3$) obtained from TGA (Fig. R9). TGA data have been added to show the purity of samples.

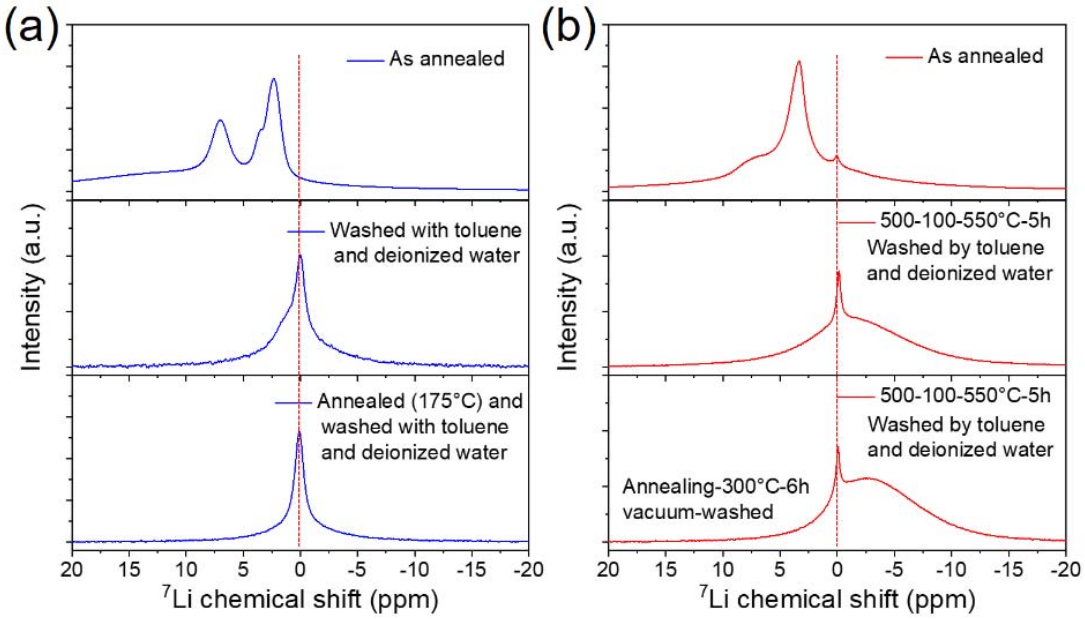


Fig. R8. $^{7}$Li MAS-NMR spectra of samples (before or after washing by toluene and deionized water, and after annealing and washing by toluene and deionized water) obtained by annealing 500 mg $C_{60}$ with 100 mg $Li_3N$ (a) at 480 °C for the $C_{60}$ polymer crystal and (b) at 550 °C for LOPC. The spectrometer frequency was 155.51 MHz for $^{7}$Li. The 90 ° pulse was 1.9 μs for Li (spin rate of 12 kHz, a repetition time (d1) of 1 s, 512 scans). The NMR signals are externally referred to a 1.0 M LiCl aqueous solution.

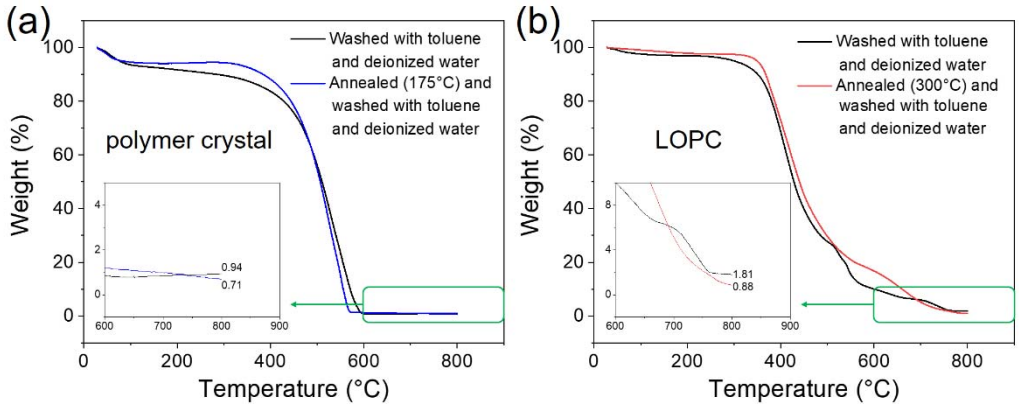


Fig. R9. Thermogravimetric analysis (TGA) of (a) the $C_{60}$ polymer crystal and (b) LOPC before or after annealing/washing under ambient atmosphere.

5) When the annealing temperature was reduced to about 480 °C the authors obtain a $C_{60}$ polymer after washing. It is not clear why this phase is formed, and the reaction conditions during the washing procedure need to be better investigated. A linear orthorhombic polymer obtained by charge transfer is normally obtained at low charge transfer (for example the $A_1C_{60}$-phases). This could be explained by either a steric hindrance at 480 °C which somehow leads to a polymerization that cannot evolve further or due to Li-remnants that develop to a doped polymer phase during the washing procedure. The authors should look into this.

**Response**: XRD spectra of the unpurified or partially purified samples have been obtained for the samples made at 480 °C (Fig. R6), indicating that a $C_{60}$ polymer crystal is formed before washing. Indeed steric hindrance could play a role. For example,, the charge transfer from Li to $C_{60}$ could be restricted by the incomplete decomposition of $\alpha$-$Li_3N$ or the poor mixing of $Li_3N$ and $C_{60}$, since our annealing time (*i.e.*, the time for diffusion of $Li_3N$/Li) is much shorter than that for the formation of $A_xC_{60}$ in previous studies (typically, several weeks).

To monitor the reactions, we have checked the XRD of samples obtained by annealing 500 mg $C_{60}$ with 100 mg $\alpha$-$Li_3N$ at 480 ºC, 550 ºC, or 575 ºC, on the dependence of annealing time. Figs. R10 and R11 show the same samples before and after washing with toluene and deionized water (*i.e.*, Figs. R10a and R11a are from the same sample before and after washing, respectively). From Figs. R10a-10c and Figs. R11a-11c, we see that a $C_{60}$ polymer crystal is already formed for an annealing time of 30 min and also for an annealing time of 300 min, at 480 ºC. Washing removes $Li_4C_{60}$, which exists for all three annealing times. From Figs. R10d-10f and Figs. R11d-11f, we can see that the structure of carbon changes from a polymer crystal to LOPC when the annealing time at 550 ºC is increased from 30 to 150 and 300 min. No $Li_4C_{60}$ is detected for the annealing time of 300 min even before washing. Figs. R10g-10i and Figs. R11g-11i show that LOPC is formed for annealing times of 30 and 150 min at 575 ° C, but becomes amorphous after 300 min. No $Li_4C_{60}$ was found at all stages.

The above experiments clearly show that the formation of a $C_{60}$ polymer crystal and LOPC is sensitive to both annealing temperature and time for a $C_{60}$/$Li_3N$ ratio of 500 mg/100mg. We suggest that the longer annealing increases the diffusion of $Li_3N$/Li into the $C_{60}$ molecular crystal and/or as formed polymer crystal, leading to the eventual formation of LOPC.

We have added the data to the revised Supplementary Information for a better understanding of the formation of LOPC.

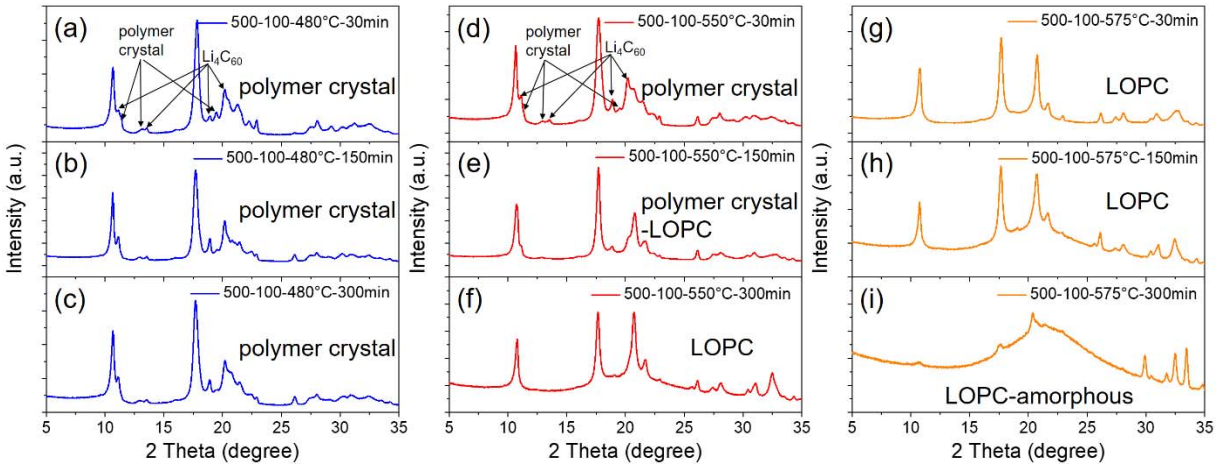


Fig. R10. Cu $K_\alpha$ ($\lambda$ = 0.15418 nm) XRD patterns of samples before washing: (a-c) polymer crystals made by annealing 500 mg $C_{60}$ with 100 mg $Li_3N$ at 480 °C for times of (a) 30 min; (b) 150 min; (c) 300 min, (d-f) materials made by annealing at 550 °C for times of (d) 30 min; (e) 150 min; (f) 300 min, and (g-i) LOPC made by annealing at 575 °C for times of (g) 30 min; (h) 150 min; (i) 300 min.

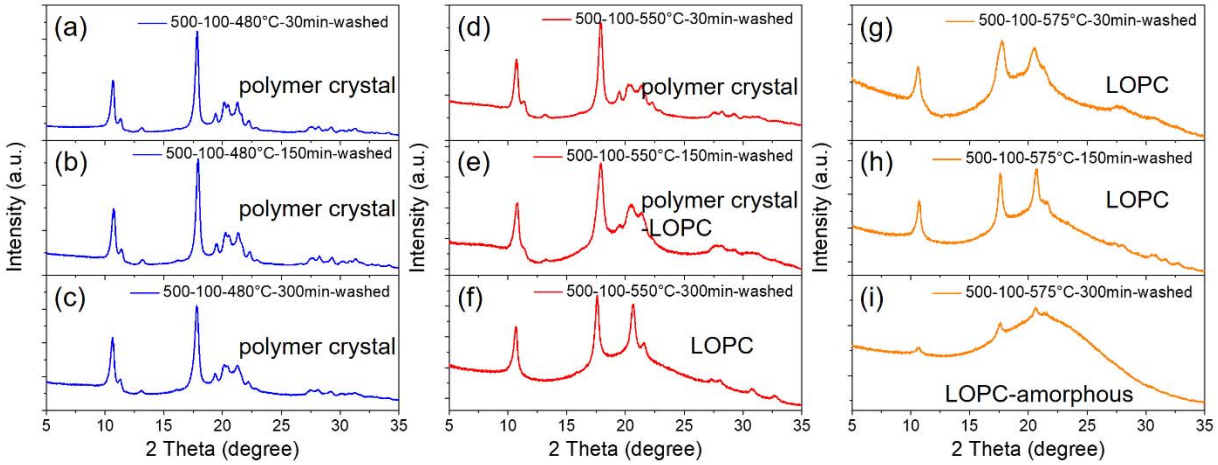


Fig. R11. Cu $K_\alpha$ ($\lambda$ = 0.15418 nm) XRD patterns of samples after washing with toluene and deionized water, (a-c) polymer crystals made by annealing 500 mg $C_{60}$ with 100 mg $Li_3N$ at 480 °C for times of (a) 30 min; (b) 150 min; (c) 300 min, (d-f) materials made by annealing at 550 °C for times of (d) 30 min; (e) 150 min; (f) 300 min, and (g-i) LOPC made by annealing at 575 °C for times of (g) 30 min; (h) 150 min; (i) 300 min.

6) The in-situ MAS-NMR should be presented so that the spinning side bands can be observed, since they would directly reveal when the $C_{60}$ becomes static. From figure S14 b this seems to occur around roughly 260 C (530 K) which would correspond perfectly with the conditions used to for the alkali-doped polymer phases (Li4C60, Na4C60…).

**Response**: Because we tried to capture the intermediate state of the reaction with *in-situ* MAS-NMR spectroscopy, the NMR acquisition time was set as ~ 12.8 min (a repetition time (d1) of 6 s, 128 scans) with a low spin rate (1.16 ~ 1.06 kHz), so the spin sidebands could not be observed. Thus, the spin sidebands in *in-situ* $^{13}$C-MAS-NMR spectra cannot be seen from 160 ppm to 120 ppm even in the enlarged portion of the spectrum at 17.5 °C. The disappearance of the 143.1 ppm $^{13}$C-peak reveals that $C_{60}$ molecules change from a state of quick rotation to static since the chemical environment of the 60 C atoms is not exactly the same for the static cage (J. *Phys. Chem. 1991, 95, 9-10*). The *in-situ* spectra in revised Fig. S21b (also repeated below) might indicate that the phase conversion happens at around 389 °C.

To compare with the conditions used for preparing the alkali-doped polymer phases, we have checked the reported reaction temperatures in the literature and list them in Table R1. They are concentrated at 480 ~ 550 K (generally 260 ° C) for the alkali-doped polymer phases ($Li_4C_{60}$, $Na_4C_{60}$…). Because our preparation was performed under conditions different from those reported in the papers listed here, we are not sure what happens at 260 °C, which is accidently close to a set temperature (~ 259.2 °C) in our *in-situ* measurements.

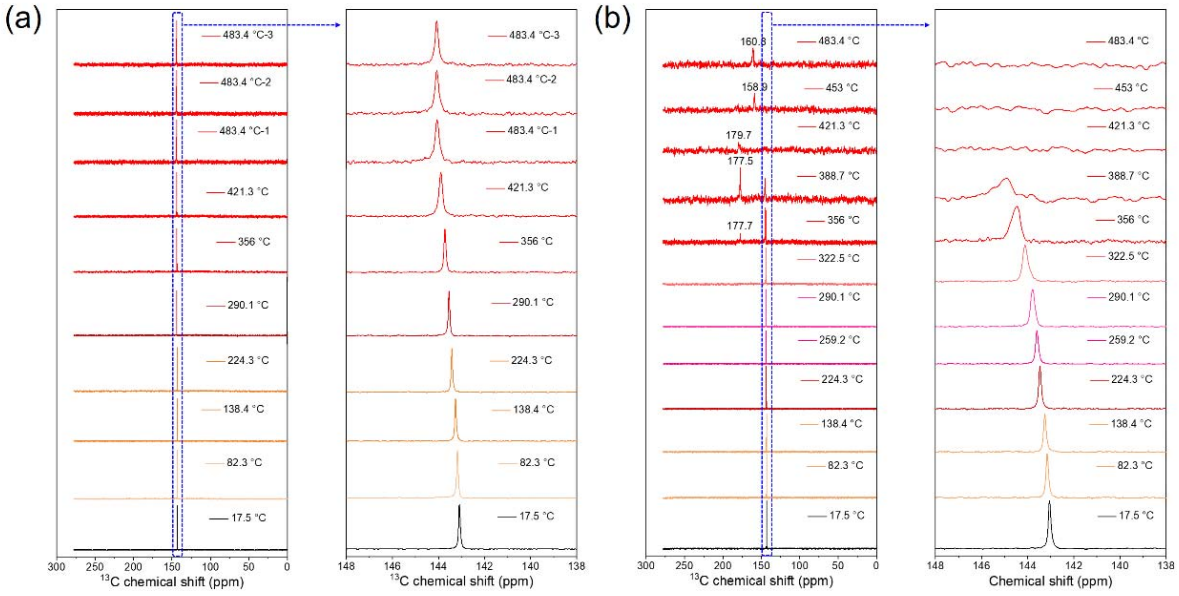


Revised Fig. S21. *In-situ* $^{13}$C MAS-SSNMR spectra of 500 mg $C_{60}$ (a) without or (b) in the presence of 100 mg $\alpha$-$Li_3N$.

Table R1. Preparation conditions of $Li_4C_{60}$, $Na_4C_{60}$ and others in related literatures.

| Samples | Li/Na/K | Temperature | Time | Ref. | Note |
|---|---|---|---|---|---|
| $Li_4C_{60}$ | $LiN_3$ | 450K, 500K | 5h | *J. Am. Chem. Soc. 2004, 126, 15032-15033.* | $LiN_3 \rightarrow Li_3N$ XRD study |
| $Li_{15}C_{60}$ | / | / | / | *AIP Conf. Proc. 2001, 591, 141-144.* | NMR study |
| $Li_{15}C_{60}$ | Enriched $^7LiN_3$ | / | / | *AIP Conf. Proc. 2001, 591, 145-148.* | Raman study |
| $Li_{12}C_{60}$ | $LiN_3$ | / | / | *Phys. Rev. B 1999, 59, 8343-8346.* | Annealed at 550K for 6h |
| $Li_{12}C_{60}$ | Pure $^7LiN_3$ | / | / | *Phys. Rev. B 2000, 61, 3404-3409.* | Neutron study |
| $Li_{x(6,12,15)}C_{60}$ | Enriched $^7LiN_3$ | 420K-480K | / | *Phys. Rev. B 2001, 63, 113405.* | Annealed at 580K for 6h |
| $Li_{x(1-6)}C_{60}$ | $Li/LiN_3$ | 540K, 510K | / | *Phys. Rev. B 2005, 72, 155437* | Several regrinding |
| $Li_{x(6-15)}C_{60}$ | Enriched $^7LiN_3$ | / | / | *J. Chem. Phys. 2001, 115, 472-476.* | NMR study |
| $Li_4C_{60}$ | / | 550K | two weeks | *J. Phys. Chem. Solids 2004, 65, 317-320.* | Ground once |
| $Li_4C_{60}$ | Follow the Phys. Rev. B 2005, 72, 155437. | | | *Phys. Rev. B 2007, 75, 081401(R).* | |
| $Li_4C_{60}$ | Follow the Phys. Rev. B 2005, 72, 155437. | | | *Phys. Rev. Lett. 2009, 102, 145901.* | |
| $Li_4C_{60}$ | Follow the Phys. Rev. B 2005, 72, 155437. | | | *Phys. Rev. B 2015, 92, 014305.* | |
| $Li_4C_{60}$ | Follow the J. Am. Chem. Soc. 2004, 126, 15032-15033. | | | *Phys. Rev. B 2016, 93, 205103.* | |
| $Li_4C_{60}$ | Follow the Phys. Rev. B 2005, 72, 155437. | | | *Carbon 2016, 100, 196-200.* | |
| $Li_4C_{60}$ | Follow the J. Am. Chem. Soc. 2004, 126, 15032-15033. and Phys. Rev. B 2007, 75, 081401(R). | | | *New Journal of Physics 2008, 10, 033021.* | |
| $Na_4C_{60}$ | / | 630K | two weeks | *J. Phys. Chem. Solids 2004, 65, 317-320.* | Ground once |
| $Na_nLi_{4-n}C_{60}$ | / | 540K | 3 weeks | *J. Phys. Chem. Solids 2004, 65, 355-357.* | Ground once a week |
| $Li_4C_{60}$ | Li | 523K | Several weeks | *J. Phys. Chem. Solids 2006, 67, 1091-1094.* | Ground once a week |
| $Na_4C_{60}$ | Na | 523K | Several weeks | *J. Phys. Chem. Solids 2006, 67, 1091-1094.* | Ground once a week |
| $Na_4C_{60}$ | Na | 630K | two weeks | *Phys. Rev. B 2002, 65, 155421.* | |
| $K_3C_{60}$ | K | 520K | two weeks | *Phys. Rev. B 2002, 65, 155421.* | |
| $Na_4C_{60}$ | $Na/NaN_3$ | 200 °C | two weeks | *Phys. Rev. Lett. 1997, 78, 4438-4441.* | Grinding |

7) I do not agree that the Raman spectra of LOPC at all matches the contour of the simulated spectrum. It is also unclear why the 1449-peak in the simulated spectra would be related to the pentagonal pinch mode. The 1455 peak in figure 1 d is also not visible, and it is therefore difficult to follow discussions on this peak.

**Response**: The simulated Raman spectrum of LOPC is sensitive to the detailed structure since all simulations have to be performed with certain LOPC structure models (Figs. R12 a to g). Since the exact atomic structure of LOPC is not yet known, an exact matching between simulation and experimental spectroscopy is, we suggest, not expected. The detected experimental Raman spectrum of LOPC may be attributed to contributions from LOPCs with slightly different atomic structures, and graphene-like structures as shown in the changes in $C_{60}$ described in Fig. 3 in the manuscript. To illustrate the point, we have taken the LOPC structures shown in Figs. S1A and S1F, combined the Raman spectra of graphene and $C_{60}$, and achieved a better matching between experimental contour and fitting curves, as shown in Fig. R11h. Note a larger Lorentz broadening of LOPCs has been used to fit the Raman spectrum. We note that there are many such kinds of combinations, all of which, however, consist of the breathing mode (~1580 $cm^{-1}$) of hexagonal rings and also the pentagon pinch mode (~1460 $cm^{-1}$) as a component.

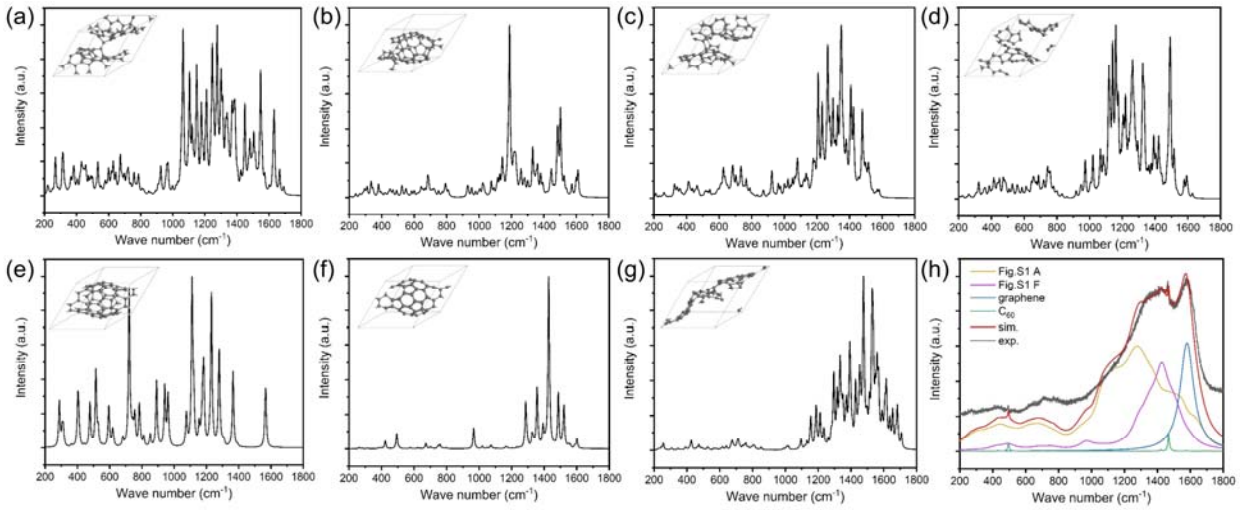


Fig. R12. Simulated Raman spectra of the LOPC structures shown in (a) Fig. S1A, (b) Fig. S1B, (c) Fig. S1C, (d) Fig. S1D, (e) Fig. S1E, (f) Fig. S1F and (g) Fig. S1H. (h) Experimental Raman spectra fitted with the LOPC structures shown in Fig. S1A and S1F, graphene and $C_{60}$. The Raman spectra of LOPCs shown in Figs. S1A and S1F are obtained by DFT simulation and the Raman spectrum of $C_{60}$ was from experimental measurement. The Raman spectrum of graphene was calculated using DFT by considering only phonons at the gamma point, resulting in one peak.

The simulated peak at 1449 $cm^{-1}$ for the LOPC structure shown in Figure 1 (also in Fig. S1A), is the stretching mode of pentagon rings, as shown in Fig. R13. A movie of showing this 1449 $cm^{-1}$ mode has been uploaded with the revised Supplementary Information. Such a mode is also close to the main $A_g(2)$ peak of $C_{60}$ and the peak at ~1473 $cm^{-1}$ in a $C_{60}$ polymer crystal, both of which are attributed to the stretching of pentagon rings according to DFT calculations.

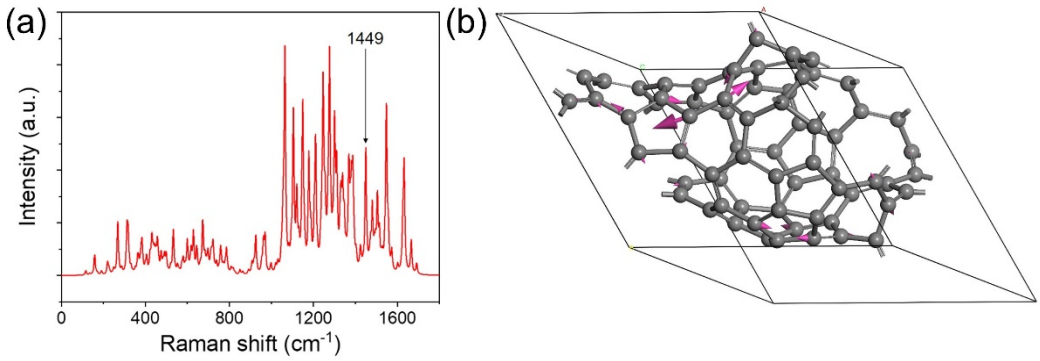


Fig. R13. (a) Simulated Raman spectrum and (b) model of the 1449 $cm^{-1}$ vibration of LOPC based on the proposed structure A in Figure S1 (proposed LOPC structure in Fig. 1a).

We have obtained more Raman spectra of two LOPC samples with laser wavelengths of 532 nm, 633 nm, and 752 nm, as shown in Fig. R14. The 1455 $cm^{-1}$ peak was visible for the laser wavelengths of 532 and 633 nm. Considering the presence of the $A_g(1)$ breathing mode (496 $cm^{-1}$), we believe that pentagons are plentiful in LOPCs, and are one of the main structural features of LOPCs.

We have revised the description and discussion of Raman spectra of LOPC in the revised manuscript with this set of new data shown in revised Supplementary Information.

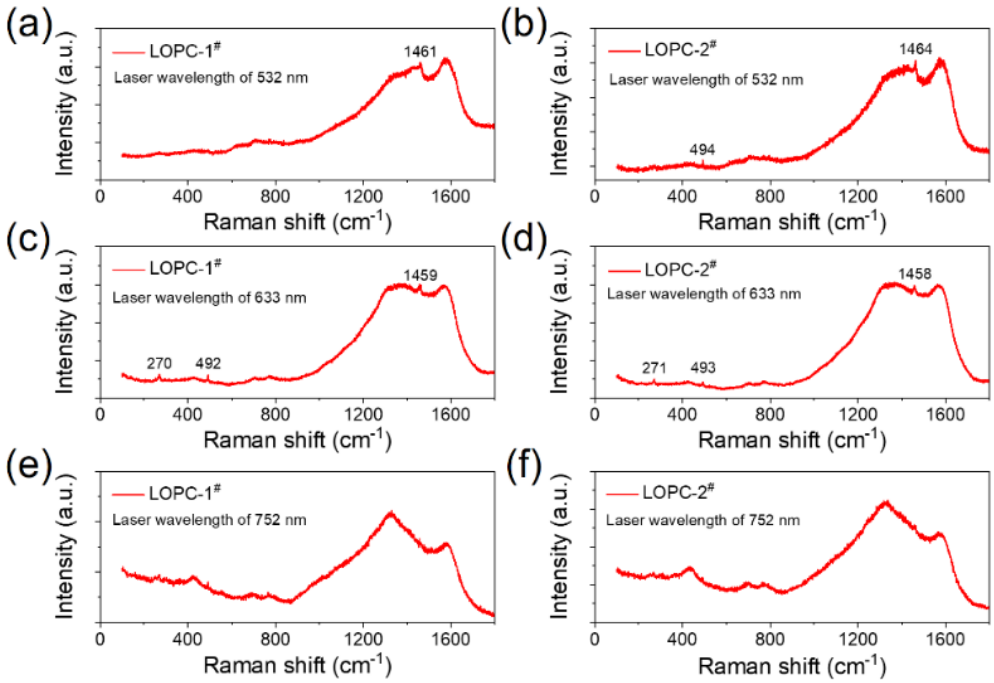


Fig. R14. (a), (b) Raman spectra for LOPCs with a laser wavelength of 532 nm (power of 500 μW, integration time of 60 s, 3x lens, grating of 1800 lines); (c), (d) Raman spectra for LOPCs with a laser wavelength of 633 nm (power of 650 μW, integration time of 60 s, 4 and 5x lens, grating of 1200 lines); (e), (f) Raman spectra for LOPCs with a laser wavelength of 752 nm (power of 700 μW, integration time of 60 s, 4 and 6x lens, grating of 600 lines).

8) The MAS-NMR reveal a $sp^3$ peak at 76 ppm. The intensity of this peak should be related to the $sp^2$ carbon (143 ppm) in order to estimate the covalent $sp^3$-bonding in the structure.

**Response**: Additional simulations of NMR chemical shift have been done by using VASP software using a linear response method. The geometrical model of a $C_{60}$ polymer crystal colored by calculated NMR chemical shift is shown in Fig. R15.

Table R2 shows the deconvolution of the experimental $^{13}C$ MAS-NMR spectrum of a $C_{60}$ polymer crystal and calculated NMR positions of C atoms under different chemical environments. We have estimated the proportion of covalent $sp^3$-bonded carbon to $sp^2$ carbon (more appropriately: trivalently bonded carbon (TBC), 143 ppm; it is not expected that TBC atoms are perfect $sp^2$-bonded, such as they are in graphene or graphite) in the $C_{60}$ crystal polymer by the intensity ratio, $I_{(sp3)}/(I_{(sp3)}+I_{(sp2)})$ and this was found to be ~ 5.3% for the $C_{60}$ polymer crystal, which is reasonably close to the simulation value of 6.7%. In comparison, a value of 5.17% was obtained from MAS NMR spectra of "the orthorhombic (1D) phase of $C_{60}$ polymer" with a spinning rate of 12 kHz and repetition time of 200 s (*Appl. Phys. A 1997, 64, 295-299*). More discussion on the content of $sp^3$ carbon has been added in the revised manuscript with data added in the revised Supplementary Information.

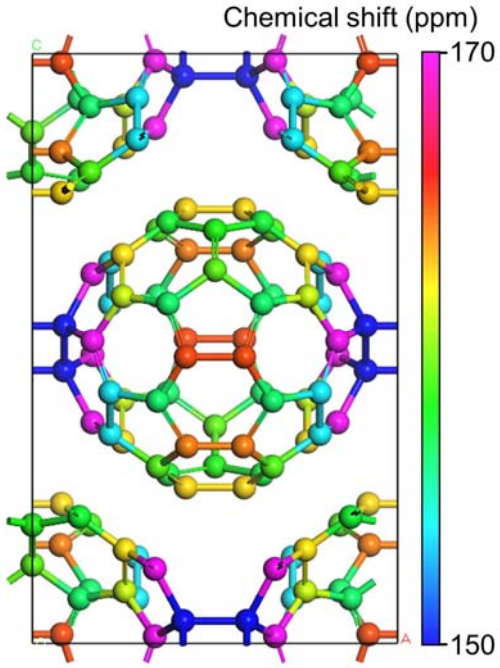


Fig. R15. The $C_{60}$ polymer crystal model colored by calculated NMR chemical shift for each atom.

Table R2. Lorentz deconvolution of $^{13}C$ MAS-NMR peaks in experimental results and calculations for the $C_{60}$ polymer crystal.

| Exp. fitting/ppm | $sp^2/sp^3$ | Relative intensity | Cal. /ppm | $sp^2/sp^3$ | Relative intensity |
|---|---|---|---|---|---|
| 149.3 | $sp^2$ | 2.37 | 171.0329 | $sp^2$ | 1 |
| 146.5 | $sp^2$ | 6.14 | 170.4294 | $sp^2$ | 1 |
| 143.9 | $sp^2$ | 6.43 | 165.0488 | $sp^2$ | 1 |
| 140.2 | $sp^2$ | 3.02 | 164.1651 | $sp^2$ | 1 |
| | | | 162.6580 | $sp^2$ | 1 |
| 76.0 | $sp^3$ | 1 | 162.4282 | $sp^2$ | 1 |
| | | | 161.0797 | $sp^2$ | 1 |
| | | | 158.9835 | $sp^2$ | 1 |
| | | | 157.4475 | $sp^2$ | 1 |
| | | | 156.5427 | $sp^2$ | 1 |
| | | | 156.4949 | $sp^2$ | 1 |
| | | | 153.8134 | $sp^2$ | 1 |
| | | | 153.7263 | $sp^2$ | 1 |
| | | | 158.1156 | $sp^2$ | 0.5 |
| | | | 159.2344 | $sp^2$ | 0.5 |
| | | | | | |
| | | | 95.9155 | $sp^3$ | 1 |
| $I_{(sp3)}/(I_{(sp2)}+I_{(sp3)})$ = 1/18.96 = 5.27% | | | $I_{(sp3)}/(I_{(sp2)}+I_{(sp3)})$ = 1/15 = 6.67% | | |

9) It would be helpful to show MAS-NMR also before washing to reveal the effect of charge transfer (which should go away after removing the Li).

**Response**: From *in-situ* $^{13}C$ MAS-NMR (Figure 3b and revised Figure S21, shown above), we may see the effect of charge transfer. At room temperature, no significant charge transfer from $Li_3N$ to $C_{60}$ was observed because the position and FWHM of $^{13}C$ peak did not change. In contrast, the appearance of new peaks at ~ 178 ppm at temperatures above 356 °C and at ~ 159 ppm at temperatures above 453 °C has been attributed to rotating $C_{60}^{(3-)}$ ions (*Science 1991, 253, 884-886*) and $C_{60}^{(6-)}$ ions (*Reviews of Modern Physics 1996, 68, 855*), indicating the obvious charge transfer from $Li_3N$/Li to $C_{60}$.

10) The MAS-NMR should be compared to the 13-C NMR obtained by [Ricco, PHYSICAL REVIEW B, Volume, 72, 15, Article Number, 1554379]. The different components in the 143-ppm band should represent $sp^2$ carbon-atoms with different chemical environment. The authors need to better correlate these to the different carbons in their structural models. It is unclear why the 140.2-peak has higher FWHM than the rest. This might indicate that a fifth peak should be added. It might be possible to correlate the MAS-NMR to the neutron scattering analysis.

**Response**: We have compared the $^{13}C$ MAS-NMR result of $C_{60}$ polymer crystal in our work with that in the reference [Ricco, PHYSICAL REVIEW B, Volume, 72, 15, Article Number, 155437], as shown in Fig. R16. We have also correlated the carbon atoms with

different chemical environments in a structural model of a $C_{60}$ polymer crystal with $^{13}C$ MAS-NMR peaks, as previously listed in Table R2.

In the reference, the original description was that "The relatively close spacing of the $sp^2$ multiplet components, along with the low spinning rate imposed by geometrical constraints, prevented us from unambiguously assigning the $sp^2$ peaks to each of the 14 structurally inequivalent $sp^2$ carbon atoms".

A similar situation exists in our work. In our simulation, 15 structurally inequivalent $sp^2$ carbon atoms (TBCs) were simulated (Fig. R15 and Table R2). For the experimental spectrum (Fig. R16a), we suggest the current fitting of 4 peaks is reasonably satisfactory. The 140.2 ppm-peak in $^{13}C$ MAS-NMR of a $C_{60}$ crystal polymer has a larger FWHM than the other three peaks, which could be contributed by multiple carbon atoms with a similar chemical environment. It is difficult to add the fifth peak into the fitting because the exact peak position cannot be determined in Fig. R15a. Note that it is challenging to ensure the accuracy of NMR peak fitting as the exact structure of LOPC cannot be determined at the atomic scale.

On the other hand, although neutron scattering analysis has shown various distances between carbon atoms, the complicated structure and the large number of atoms in polymer crystals (compared to oligomers) have made the correlation between MAS-NMR and neutron scattering extremely challenging. But with purer samples, higher resolution neutron scattering and $^{13}C$-MAS-NMR performed at low temperatures, the relationship could likely be determined in future studies.

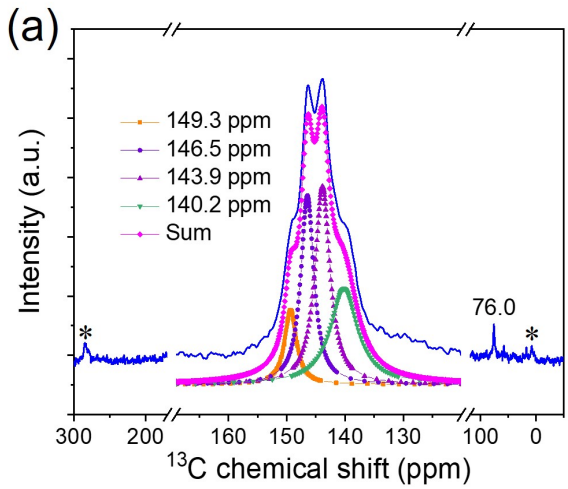


**[REDACTED]**

Fig. R16. (a) $^{13}C$ MAS-SSNMR spectrum of $C_{60}$ polymer crystal (room temperature, spinning rate of 12 kHz and a repetition time (d1) of 200 s, 1024 scans). Inset shows the Lorentz fitting of peaks (at 140.2, 143.9, 146.5 and 149.3 ppm); * shows the spin sidebands; (b) **[REDACTED]**

11) Li-7 MAS-NMR, as performed in [Journal of Physics and Chemistry of Solids 67 (2006) 1091–1094] before washing would be able to reveal the location of the Li-atoms, and thus also explain better the mechanism of the polymer/cage breaking formation.

**Response**: We have carried out additional $^{7}$Li MAS-NMR testing (based on methods described in the Journal of Physics and Chemistry of Solids 67 (2006) 1091–1094) and show the experimental spectra with Lorentz fitting in Fig. R17, for the samples obtained by annealing 500 mg $C_{60}$ with 100 mg $Li_3N$ at 480 °C or 550 °C before washing by toluene or deionized water.

By taking the values reported in the literature (*J. Phys. Chem. Solids 2006, 67, 1091–1094*), we can see that the signal of Li at the **O**-site is close to the signal of Li at the **T**-site in the as-annealed sample of the $C_{60}$ polymer crystal. In contrast, the signal of Li in the **O**-site is significantly greater than the signal of Li in the **T**-site for the as-annealed sample of LOPC.

Because our additional AIMD simulations shown in Fig. R5 have indicated the possibility of Li occupation at the **T'** site, we also simulated the chemical shift of Li by DFT calculations, showing 7.9 ppm for the **O** site, 1.6 ppm for the **T** site, and 1.5 ppm/3.2 ppm for the **T'** site along the polymer bonding direction and vertical to the polymer bonding direction. That is, NMR peak(s) of Li at the **T'** site overlap peaks from the **T** and **O** sites. We or others may be able to further clarify the positions of Li by using higher resolution NMR and better controlled samples in future studies.

In the revised manuscript we have given a deeper account of the introduction of Li from *α*-$Li_3N$, breaking of $C_{60}$ molecules with more Li and different $^{7}$Li NMR in LOPC compared to that in polymer crystal, for a better understanding of LOPC formation.

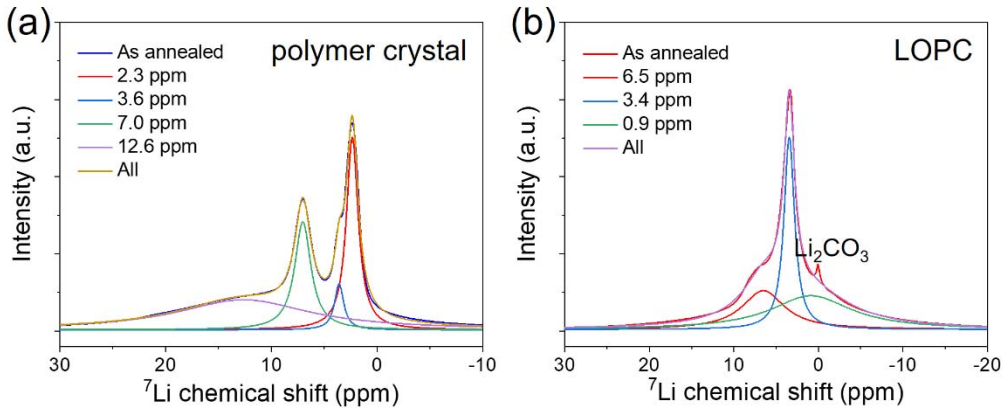


Fig. R17. $^{7}$Li MAS-NMR spectra and Lorentz fitting of samples (without any washing) obtained by annealing 500 mg $C_{60}$ with 100 mg $Li_3N$ (a) at 480 °C for the polymer crystal or (b) at 550 °C for LOPC.

12) The resistance measurements are not well-described. First of all the resistance to high extent will be dominated by grain boundaries. What are the sizes of the "crystalline domains" as determined from XRD and FFT? In total there are still a number of issues that need to be clarified before a decision can be made on the suitability of the manuscript to be published.

**Response**: We measured the conductivity of the original $C_{60}$, LOPC and the polymer crystal powders using the adhesive (PTFE) method. The result in Fig. 4c shows that the LOPC powder is metallic. We also tested the conductivity-temperature curve of LOPC powder using the tablet pressing method (Fig. 4d). The influence of contact resistance between adjacent particles is minimized by comparing the measurements with those performed on graphite or graphene powders.

In addition, we have tried to measure the electrical conductivity of individual LOPC particles (LOPC-550°C-5h, LOPC-560°C-5h, LOPC-575°C-5h and LOPC-600°C-5h, all made by annealing 500 mg $C_{60}$ with 100 mg $\alpha$-$Li_3N$) with a four-probe method performed at temperatures from 300 to 2 K. The measurements of two samples (LOPC-575°C-5h and LOPC-600°C-5h) were successful and the results are shown in Fig. R18. For the particle of LOPC-575°C-5h (Fig. R18a), the resistance increases from 0.11 Ω to 0.28 Ω when the temperature decreases from 300 K to 3 K (Fig. R18c), demonstrating a semiconducting behavior. For the particle of LOPC-600°C-5h (Fig. R18b), the resistance firstly increases till 8 K and then decreases (Fig. R18d). Such a 'kink' of resistance dependence is considered to be related to the amorphous structure of LOPC-600°C-5h (refer to the XRD pattern in Fig. 1c in the manuscript), which may cause the hopping of electrons because of defects or less conjugated carbons. We notice that a similar kink has been observed in the resistivity measurement performed across the layers of highly oriented pyrolytic graphite; no kink was observed for the in-plane measurements (*Phys. Rev. B 1987, 35, 4483-4488*). These results are consistent to the results based on compressing the powders that is presented in the manuscript.

To determine sizes of the "crystalline domains", the Debye-Scherrer formula $D = \frac{K\gamma}{B\cos\theta}$ ($K$ is the Scherrer constant, 0.89; $\gamma$ is the wavelength of the X-rays, 0.15418 nm; $B$ is the full width at half maxima (FWHM) of diffraction peaks (rad); $\theta$ is the Bragg diffraction angle (in °)) has been used to roughly estimate the average sizes of "crystalline domains". Calculated $D$ values using the FWHMs of the (111), (220) and (311) diffraction peaks were 26.9 nm, 24.5 nm and 24.3 nm, respectively, much smaller than the size of the particles.

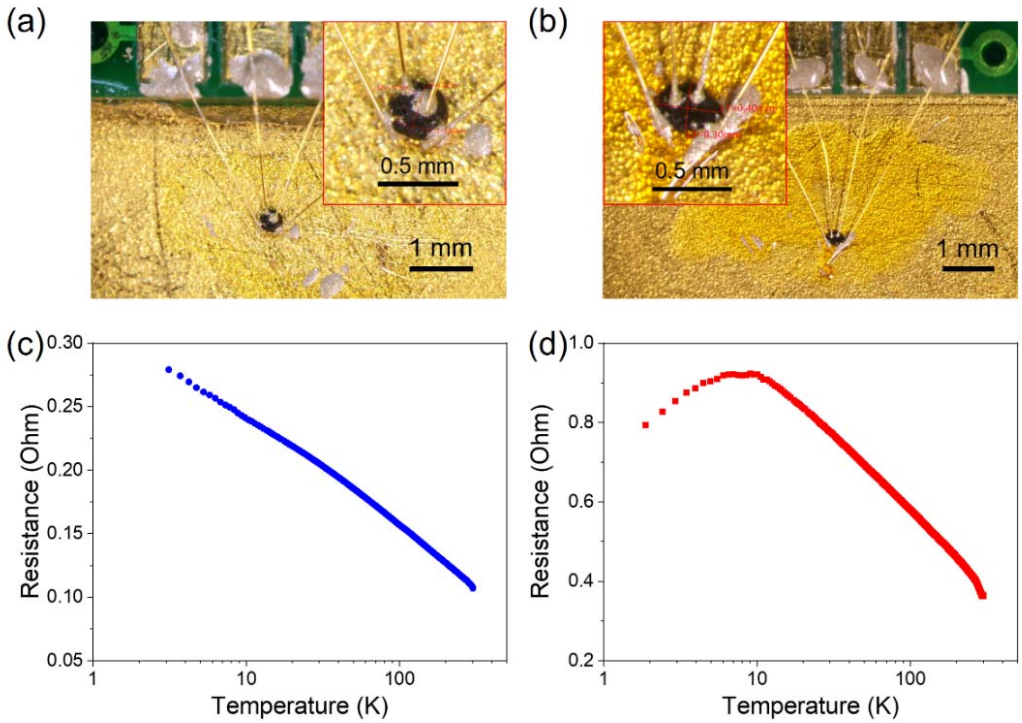


Fig. R18. Temperature-dependent resistance measurements for particles of (a, c) LOPC-575°C-5h and (b, d) LOPC-600°C-5h.

Referee #2 (Remarks to the Author):

In our traditional knowledge of crystallography, solid-state materials are categorized by their structures into three types, e.g., crystalline (having periodic translation symmetry), amorphous (no periodic and orientational symmetry), and quasi-crystalline (having orientational but not periodic translation symmetry) phases. Ten years ago, Wang et al. (Science 2012, 337, 825) first discovered a hexagonal close-packed long range ordered amorphous carbon clusters through the direct high pressure transformation of $C_{60}$ using a diamond anvil cell. The discovery changes our long term understanding of the inherent disorder (amorphous building block) that cannot be present in a crystal (Science 2012, 337, 812). Unfortunately, the quantity of the sample obtained under high pressure is very limited, usually in a scale of milligrams or less, and therefore hinders the further explorations on their properties and potential applications. The present paper reports the first long range ordered porous carbon (LOPC) in a face centered cubic lattice, which can readily be produced using a chemical protocol in gram-scale at room pressure and moderate temperature. This tremendous step opens new opportunities for use of the products in new ways, and also for doing further chemistry on the products to generate other downstream products that might have interesting properties and functionalities.
The gram-scale LOPC is prepared from $C_{60}$ powder with electron transfer from $\alpha$-$Li_3N$ at 550 °C and ambient pressure. It was clearly determined that LOPC consists of connected 'broken' $C_{60}$ cages that however maintain long-range periodicity using a variety of characterizations including X-ray diffraction, Raman spectroscopy, magic angle spinning solid state nuclear magnetic resonance spectroscopy, aberration-corrected transmission electron microscopy, and neutron scattering. The simulations based on neural network show that LOPC is a metastable structure in the evolution from fullerene type to graphene type carbons, providing an understanding of the transformation from $C_{60}$ to LOPC. In my opinion, the result presented in the paper is convincing and of great importance to the fields of crystallography and materials science. It deserves to be published in Nature if the following issues/comments could be well addressed.

**Response**：Thank you for reviewing our manuscript.

1. About XRD:

It is known from the structure of long range ordered carbon clusters that the atomic structure and orientation of the crushed C60 clusters are not identical to each other. So, the x-ray diffraction of the LOPC should have two contributions: sharp diffraction peaks from fcc lattice and diffused hump from local disordering. This coexistence is clearly seen in the XRD date (figure 1b and 1c) and is crucial for the conclusion made in the paper. In the simulated XRD, there are two obvious extra peaks (at ~12.5 and ~24 degree) as compared to the measured one in figure 1b. How was the simulation carried out, and what is the structural model used in the simulation? I guess the identical carbon clusters are used in the simulation, in such a case the two extra diffraction peaks will appear because of large structure factor. In fact, the atomic structure of crushed C60 should be disorder

and the orientation must be somehow random. The authors need to point it out and add a short discussion in revision.

**Response**: The simulated XRD of the LOPC structure is obtained based on a specific carbon crystal model with 69 carbon atoms per unit cell, shown in the inset of Fig. 1a and Fig. S1A. Indeed, as the reviewer indicated, a small periodic model would lead to the appearance of two extra diffraction peaks. We agree that LOPC should contain short-range disorder, as the periodic order may be broken in some particular directions.

We have attempted to do XRD refinement to see if we can further optimize the structural model to obtain a better match with the experimental XRD. Fig. R19a shows the result from Pawley refinement. Although we can see a better fitting with experimental results, the intensity of Bragg reflections was taken as a free parameter, which can be directly changed during the refinement, thus we prefer to think it is more of a 'mathematical trick' than a real indication of structures. Rietveld refinement, as shown in Fig. R19b, which was used in combination with considering energy with the *COMPASS II force field*, has shown us a slightly modified structure with reasonable energy and fit in XRD. We can see that the two structures only have minor differences while the main structural features are maintained. However, the structure given by Rietveld refinement is not at local minima according to *DFT calculations*, and has a higher energy (~0.2 eV per atom).

We suggest the DFT optimized structure at local minima is the most reasonable choice as a metastable structure, which shows a reasonably good fitness with experimental data, yet with two extra peaks. The extra peaks might be eliminated in a large model but we are finding the computational cost (time) of such a calculation to be completely prohibitive.

Rietveld refinement has been added in the revised manuscript.

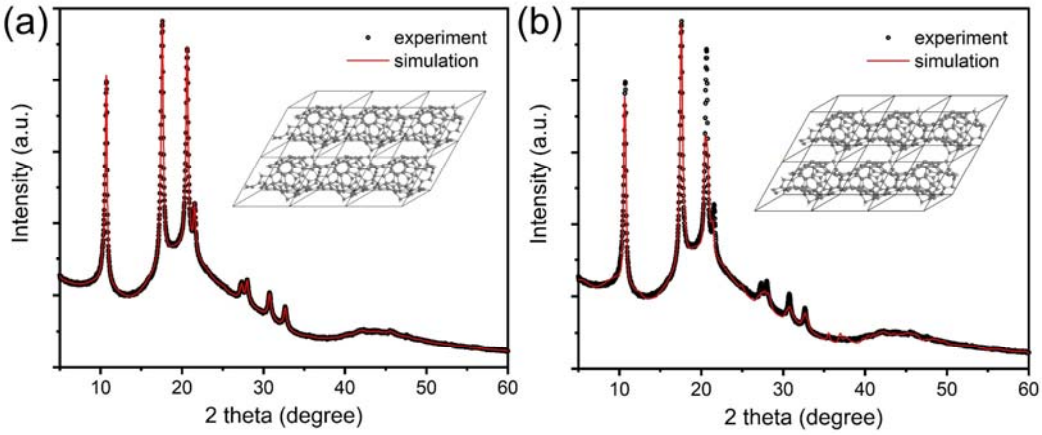


Fig. R19. XRD refinement for a representative LOPC structure by (a) the Pawley method and (b) the Rietveld method.

2. About Raman spectrum

Pristine $C_{60}$ has ten Raman modes including 8 $H_g$ and 2 $A_g$. However, there several unknown peaks exist in the Raman spectrum shown in Fig. 1a, which should be clarified. The Raman peaks of the $C_{60}$ polymer should be indexed as well.

**Response**: We have labeled prominent peaks in the experimental Raman spectra of the original $C_{60}$ and the $C_{60}$ polymer crystal (revised Fig. 1d), as repeated below. Table R3 lists all the peaks, among which those in blue have been marked in revised Fig. 1d; 4 peaks in red (in Table R3) were not observed in Ref. 2 (*Phys. Rev. B 2000, 61, 11936-11945*), but are in good agreement with our calculation results, as shown in Fig. R20 and Table R3.

More data has been added in the revised Supplementary Information.

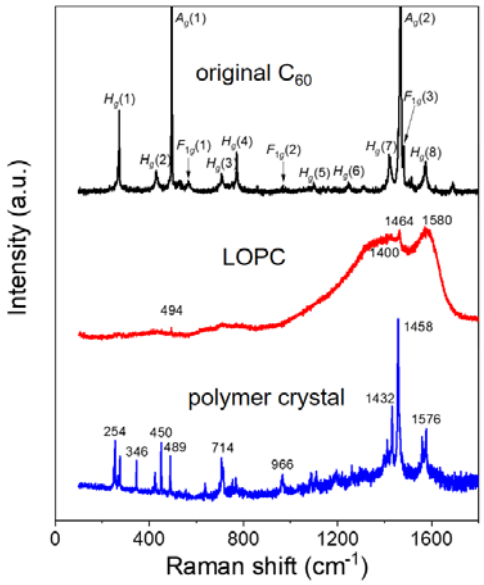


Revised Fig. 1. d) Raman spectra for the original $C_{60}$, LOPC and the polymer crystal.

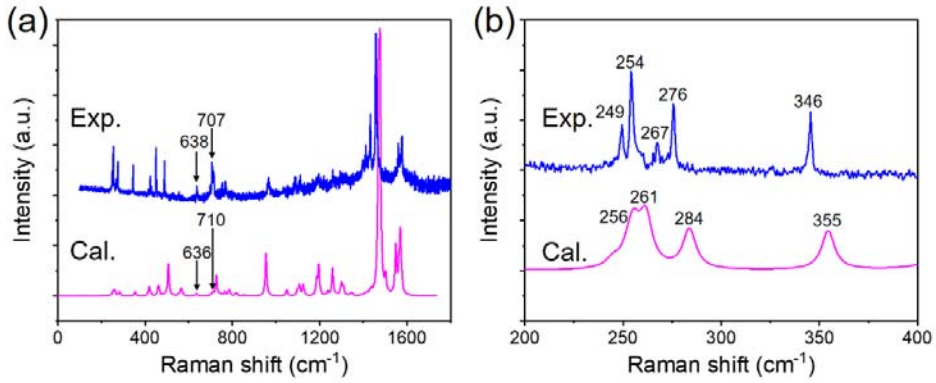


Fig. R20. Experimental and calculated Raman spectra for the $C_{60}$ polymer crystal (a) 0 $cm^{-1}$ ~ 1800 $cm^{-1}$ and (b) 200 $cm^{-1}$ ~ 400 $cm^{-1}$.

Table R3. Detailed Raman modes of the original $C_{60}$ and the polymer crystal.

| original $C_{60}$ | | | polymer crystal | | |
|---|---|---|---|---|---|
| Raman mode | Exp. position/$cm^{-1}$ | Ref. 1 position/$cm^{-1}$ | Raman mode | Exp. position/$cm^{-1}$ | Ref. 2 position/$cm^{-1}$ |
| $A_g(1)$ | 495 | 495 | / | / | / |
| $A_g(2)$ | 1468 | 1470 | / | 1458 | 1457 |
| $H_g(1)$ | 266, 272 | 267, 272 | / | 254 | 256 |
| $H_g(2)$ | 430 | 431 | / | 276 | 274 |
| $H_g(3)$ | 708 | 709 | / | 346 | 346 |
| $H_g(4)$ | 772 | 775, 778 | / | 424 | 427 |
| $H_g(5)$ | 1101 | 1102 | / | 450 | 452 |
| $H_g(6)$ | 1250 | 1252 | / | / | 471 |
| $H_g(7)$ | 1419, 1425 | 1418, 1425 | / | 489 | 488 |
| $H_g(8)$ | 1575 | 1567, 1576 | / | 556 | 556 |
| $F_{1g}(1)$ | 567 | 568 | / | 568 | 566 |
| $F_{1g}(2)$ | 969 | 973 | / | / | 577 |
| $F_{1g}(3)$ | 1480, 1482 | 1479, 1484 | / | / | 596 |
| $H_g(1)※H_g(7)$ | 1690 | 1693 | / | / | 614 |
| $H_g(1)※G_g(5)$ | 1618 | 1619 | / | / | 668 |
| $F_{2g}(1)※F_{1g}(2)$ | 1514 | 1516 | / | / | 676 |
| $F_{2u}(5)$ | 1311 | 1310 | / | 698 | 697 |
| $H_g(2)※H_g(2)$ | 860 | 862 | / | 714 | 714 |
| $H_g(1)※H_g(1)$ | 531 | 533 | / | 754 | 753 |
| | | | / | 768 | 770 |
| | | | / | / | 853 |
| | | | / | / | 945 |
| | | | / | 966 | 965 |
| | | | / | 1038 | 1040 |
| | | | / | 1089 | 1086 |
| | | | / | 1111 | 1109 |
| | | | / | 1195 | 1192 |
| | | | / | / | 1243 |
| | | | / | 1262 | 1260 |
| | | | / | / | 1297 |
| | | | / | / | 1310 |
| | | | / | / | 1350 |
| | | | / | 1398 | 1396 |
| | | | / | 1432 | 1432 |
| | | | / | 1561 | 1560 |
| | | | / | 1576 | 1572 |
| | | | / | 707 | / |
| | | | / | 638 | / |
| | | | / | 267 | / |
| | | | / | 249 | / |

Note: Ref. 1 is *Phys. Rev. B 1994, 50, 173-183*; Ref. 2 is *Phys. Rev. B 2000, 61, 11936-11945*.

3. Low-pressure adsorption/desorption

Many experimental details are missing in either the manuscript or supplementary. For example, the caption of figure 1f says “low-pressure Ar (87.3K) ...”, but with no description. Is the absorption/desorption measurement carried out at low temperature? 87.3 K is almost the liquidizing temperature of Ar.

**Response**: We have examined all experimental details in either the manuscript or supplementary information, and added any that were missing or incomplete. The absorption/desorption measurements of LOPCs were carried out at 87.3 K, which is the boiling point of liquid Ar, using the standard BET method.

4. The thermal stability:

More characterizations of TGA and mass spectrum are encouraged to be added. Mass spectrum and TGA studies on the LOPC could provide solid evidence of its characteristics. They will put more weights on the reliability of the conclusion made.

**Response**: We have carried out additional thermogravimetric analysis (TGA, in nitrogen atmosphere) and mass spectroscopy (MALDI-TOF-MS, in toluene) of the original $C_{60}$, LOPC and the polymer crystal, as shown in Figs. R21 and R22, respectively. From the TGA, we can see that LOPC has a higher stability than the original $C_{60}$ and the polymer crystal.

From the mass spectra, we estimate that the relative amounts of residual $C_{60}$ molecules (719.9-signal) in LOPC and the polymer crystal are 3.35% and 2.98%, respectively, when calculated by comparing the intensities of the $C_{60}$ and $K^+$ peaks, or 0.67% and 1.01% when calculated by comparing the intensities of the $C_{60}$ and $Na^+$ peaks (It is assumed that the ionization efficiency of the three samples and the other test conditions are completely same.). The 257.1-signal in LOPC thus might come from the broken $C_{60}$ species.

We have added the data to the revised Supplementary Information.

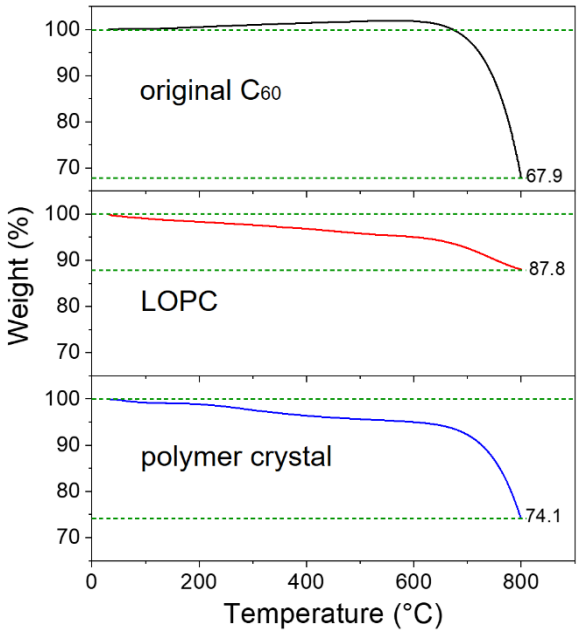


Fig. R21. Thermogravimetric analysis (TGA) of the original $C_{60}$, LOPC and the polymer crystal in nitrogen.

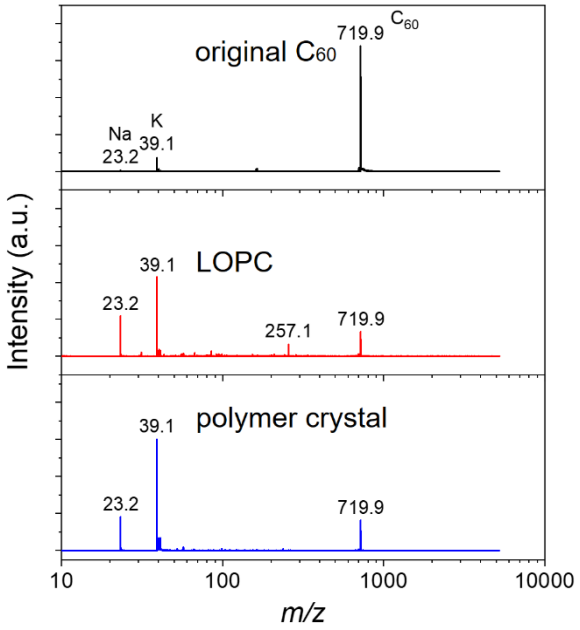


Fig. R22. MALDI-TOF Mass spectra (MS) of the original $C_{60}$, LOPC and the polymer crystal using toluene as solvent. Note that the peaks at *m/z* positions 23.2 and 39.1 were caused by residual sodium ($Na^+$) and potassium ($K^+$) ions in the solvent.

5. The application of battery:

As seen from figure S19, LOPC does not show obvious superior advantage in the application as an anode for lithium and sodium ion batteries. I would like to suggest the author to remove the last sentence of the article: “As an example, LOPC has shown potential applications ...”, as the discovery of the first fcc LOPC and the gram-scale yield are already importance enough for its publication in a prestigious journal like Nature.

**Response**: Yes, we agree. We removed: “As an example, LOPC has shown potential applications ...” in the Manuscript and Figure S19 in the Supplementary Information. Correspondingly we have removed the measurement method and data from original submission. We will further explore the properties and possible applications of LOPC in future studies.

6. Writing and organization of the paper:

The results in the paper are important and convincing. However, it is not a well written and organized paper. I think it must be easy for the authors especially the native speaker in the list to help this out.

**Response**: We have the revised manuscript professionally edited by Prof. Peter Thrower.

7. Format of references:

It is realized that format of the cited references are incorrect. It should be taken care of according to the requirement of the journal Nature.

**Response**: We have revised it as Nature format.

Referee #3 (Remarks to the Author):

In the Manuscript titled: “Long-Range Ordered Porous Carbon from $C_{60}$” Pan F. and collaborators claim the discovery of a new type of carbon. The authors report a simple and scalable method involving mixing $\alpha$-$Li_3N$ with $C_{60}$ and heating at 550 °C followed by some purification steps. Currently, the synthesis method is capable of producing large batches around one gram per batch and can be easily scaled to kilograms of more.
The building blocks for this new material are damaged $C_{60}$ cages interconnected by $sp^2$ carbon-carbon links. Some of the properties of the material are compared with pristine $C_{60}$ powders and $C_{60}$ polymer crystal which are closely related forms of carbon. The authors perform an extensive characterization of the crystalline structure of the material by several techniques including X-Ray diffraction, aberration corrected transmission electron microscopy and Raman spectroscopy and confirm that the broken C60 cages exhibits a long-range arrangement. In this study the authors find that this is a metastable form of carbon between $C_{60}$ and graphene.

A characterization of the electrical conductivity of the material to results on a value of $1.17x10^{-2}$ S $cm^{-1}$, representing an enhancement of several orders of magnitude when compared with pristine $C_{60}$ or $C_{60}$ polymer crystal. Low temperature electrical characterization revealed a possible transition from semiconductor to metallic properties as LOPC is synthesized at higher temperatures.

The manuscript shows a novel form of synthetic carbon and a very detailed characterization of the crystalline structure, as well as computational exploration of its electronic structure. However, the manuscript is presented in a form that makes it appealing mostly to the carbon science and the materials science communities, but not for a broader audience; the manuscript lacks of an outstanding property, a specific application or the explanation of the extreme importance of this discovery, because of that, I don’t believe its suitable for publication in nature.

**Response**: Thank you for reviewing our paper.
We are exploring more properties and applications of $C_{60}$ polymer crystal and LOPC, since large-scale preparation has been achieved in our methods.
For example, we have tried to characterize the electrical conductance of individual LOPC particles as a function of temperature and magnetic field intensities, with a four-probe method. As stated previously (please see Fig. R18 above), among 4 samples (LOPC-550°C-5h, LOPC-560°C-5h, LOPC-575°C-5h and LOPC-600°C-5h), two samples (LOPC-575°C-5h and LOPC-600°C-5h) have been successfully measured (the other two samples broke (were crushed) into too small species during repeated annealing and ultrasonic washing) and the results are shown in Fig. [REDACTED]. From Fig. [REDACTED] we can see that the resistance of LOPC-575°C-5h shows a monotonic decrease when the temperature decreases, in contrast to the ‘kink’ observed for LOPC-600°C-5h. Fig. [REDACTED] shows that the ‘kink’ temperature of LOPC-600°C-5h is higher for higher applied magnetic field,accompanied by a decrease in the peak resistance. A deeper understanding of the

electrical properties of LOPCs including in the presence or absence of a magnetic field, is likely to be obtained in the future.

[REDACTED]

In our recent preliminary effort, we synthesized a crystal with size of ~ 500 μm and observed the presence of polymer crystal after annealing the crystal with α-$Li_3N$ (shown in Fig. R24). At the current stage of our efforts, we have not been able to fully control the transition of the whole crystal uniformly from $C_{60}$ molecular crystal to polymer crystal and LOPC. We expect to investigate its detailed surface structure with STM and its other basic properties based on better-controlled samples in our future studies.

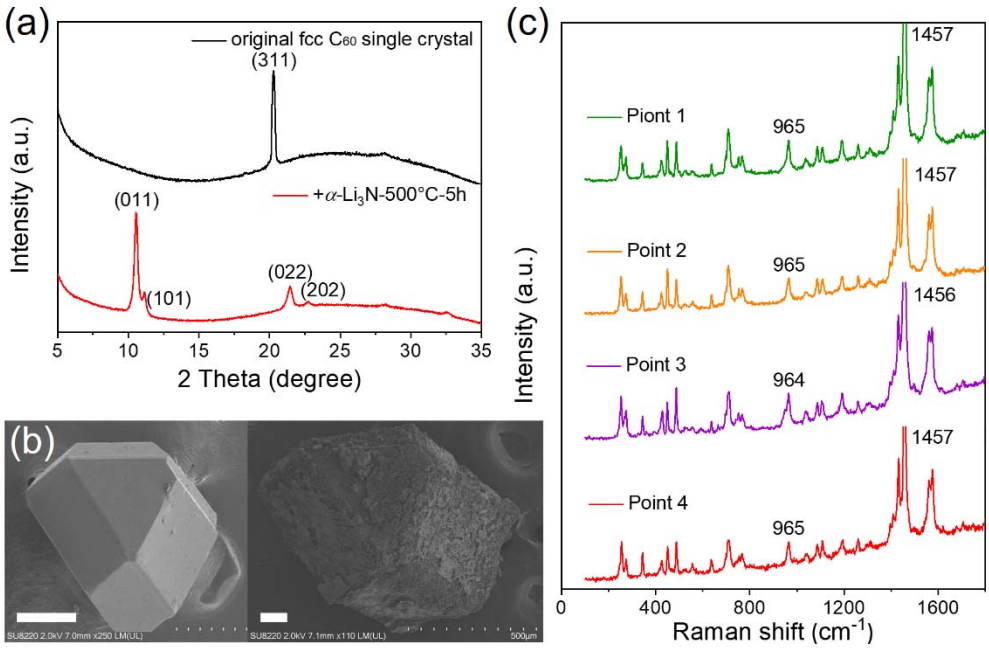


Fig. R24. (a) XRD patterns and (b) SEM images (scale bar: 100 μm) of and the original fcc-$C_{60}$ single crystal and the product (the $C_{60}$ polymer crystal) annealed at 500 °C for 5 h in Ar where the crystal is covered by *α*-$Li_3N$ powder. (c) Raman spectra of above annealed product at 4 different positions, all with the $sp^3$ characteristic peak. The SEM image before annealing shows a clean and flat surface, while the SEM image of annealed crystal shows surface restructuring.

We keep learning more about our LOPCs. For example, femtosecond transient adsorption (TA) spectra of a pure $C_{60}$ polymer crystal and LOPC in ethanol have been compared, as shown in Fig. [REDACTED]. The strong ground-state bleaching (GSB) signals of the $C_{60}$ at 525 nm (Fig. [REDACTED]) and the polymer crystal at 575 nm (Fig. [REDACTED]) might be ascribed to the formation of a doublet excited state of molecules on the surface of the sample (*J. Am. Chem. Soc., 2015, 137, 8769−8774; J. Am. Chem. Soc., 2020, 142,4411−4418*), which however did not occur in LOPC (Fig. [REDACTED]), due to the connection of broken $C_{60}$ molecules. The results are consistent to those obtained from NEXAFS and electrical conductivity measurements.

[REDACTED]

Since the original submission of our manuscript, we have been investigating the applications of LOPCs in energy storage, *e.g.*, as the anode for lithium ion batteries (LIBs) or sodium ion batteries (SIBs). Fig. R26 repeats the performance of LOPC made by annealing 500 mg $C_{60}$ with 100 mg $Li_3N$ at 550°C for 5h, as included in the last submission. By optimizing the preparation conditions, Fig. R27 below shows that the specific capacity of LOPC by annealing 500 mg $C_{60}$ with 250 mg $Li_3N$ at 500°C for 3h, reaches 350 mAh $g^{-1}$ with a great rate performance as anode of SIBs. We plan to investigate more applications of LOPCs such as in $CO_2$ adsorption, hydrogen storage, ion sieving, and catalyst loading. In the current manuscript, we have focused on the preparation and characterizations of LOPCs, and thus defined them as a new type of carbon.

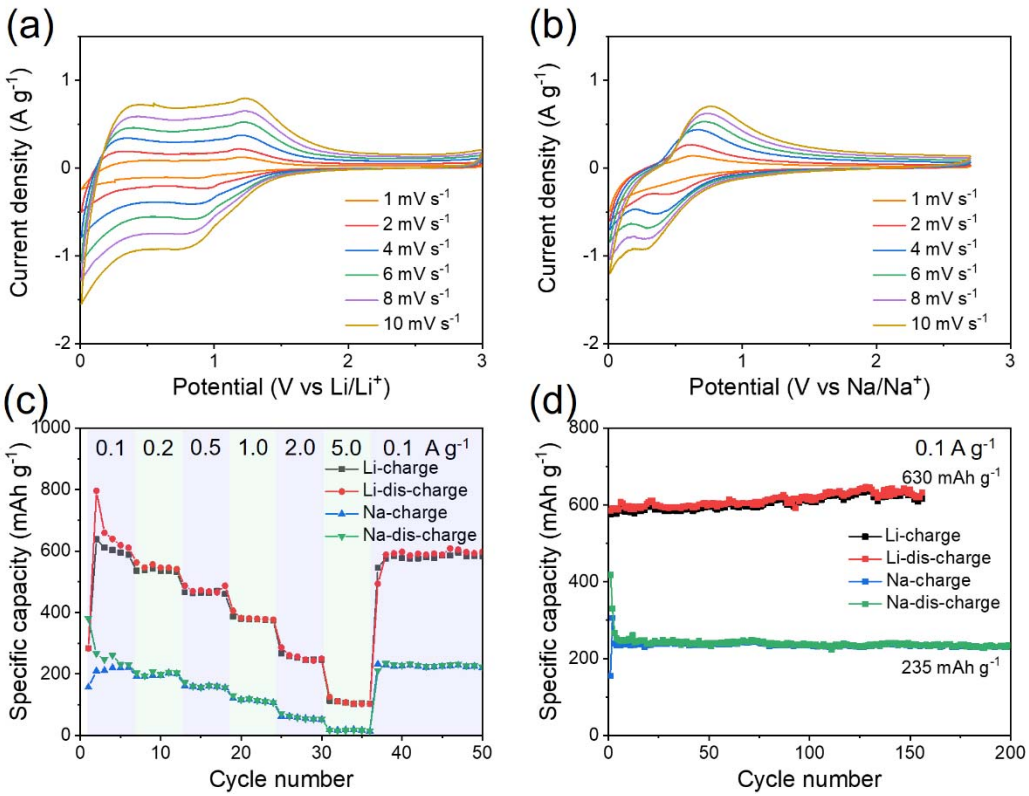


Fig. R26. Performance of LOPC (500 mg $C_{60}$-100 mg $Li_3N$-550°C-5h, washed with toluene and deionized water, annealed under vacuum at 300 °C for 6 h (3 times), washed with toluene and deionized water) as the anode for LIBs and SIBs. (a) CV (cyclic voltammetry) curves in a half-cell with a 1 m $LiPF_6$ in EC/DEC electrolyte; (b) CV curves in a half-cell with a 1 M $NaPF_6$ in EC/DMC electrolyte; (c) Rate performance at current densities from 0.1 to 5.0 A $g^{-1}$; (d) Cycling performance at a current density of 0.1 A $g^{-1}$.

[REDACTED]

**Reviewer Reports on the First Revision:**

Referees' comments:

Referee #1 (Remarks to the Author):

The authors have made a very serious review, following the remarks and suggestions made by all reviewers. By the revision they have clarified questions and doubts that existed in the previous version. The results are now convincing and of very high importance. Because of this, I think that the paper now should be accepted for publication in Nature.

Referee #2 (Remarks to the Author):

The authors have addressed my comments in a proper manner and made corresponding changes in the whole manuscript. I am glad to see all the experimental and calculating evidences are pointing to the important result of the manuscript. I think it is the time to consider the publication of the manuscript in the journal seriously.
Besides, I have few minor comments for the authors to consider.
1.The description in line 80-81, i.e. “Long-range ordered carbon clusters or super hard amorphous carbon produced by the HPHT processing of C 60 crystals have been reported.” is not proper, as the long-range ordered carbon clusters are not produced by HPHT. It could be divided into two sentences, e.g. “Long-range ordered carbon clusters, a unique crystalline material made of amorphous building blocks have been synthesized by crushing C60 cages at HP and room temperature. Superhard amorphous carbon materials produced by HPHT processing of C60 crystals have also been reported.”
2.The Raman spectra of LOPC synthesized at different conditions ranging from 500 to 575 °C are expected to be present either in the article or supplementary.

Referee #3 (Remarks to the Author):

The revised version of the manuscript makes it much easier to understand the importance of this synthetic method to produce macroscopic amounts of LOPC from C60.

I recommend it for publication in its present form.

Referee #2 (Remarks to the Author):

The authors have addressed my comments in a proper manner and made corresponding changes in the whole manuscript. I am glad to see all the experimental and calculating evidences are pointing to the important result of the manuscript. I think it is the time to consider the publication of the manuscript in the journal seriously.

Response: Thank you for reviewing our revised paper.

Besides, I have few minor comments for the authors to consider.

1.The description in line 80-81, i.e. “Long-range ordered carbon clusters or super hard amorphous carbon produced by the HPHT processing of $C_{60}$ crystals have been reported.” is not proper, as the long-range ordered carbon clusters are not produced by HPHT. It could be divided into two sentences, e.g. “Long-range ordered carbon clusters, a unique crystalline material made of amorphous building blocks have been synthesized by crushing $C_{60}$ cages at HP and room temperature. Superhard amorphous carbon materials produced by HPHT processing of $C_{60}$ crystals have also been reported.”

**Response:** Thank you. The description in line 80-81 has been revised to “Long-range ordered carbon clusters, a unique crystalline material made of amorphous building blocks have been synthesized by crushing $C_{60}$ cages at high pressure and room temperature. Superhard amorphous carbons produced by HPHT processing of $C_{60}$ crystals have also been reported”.

2.The Raman spectra of LOPC synthesized at different conditions ranging from 500 to 575 °C are expected to be present either in the article or supplementary.

**Response:** We have obtained Raman spectra of carbons prepared by annealing 500 mg $C_{60}$ with 100 mg $\alpha$-$Li_3N$ for 5 h at different temperatures ranging from 500 to 575 °C, as shown in Fig. R1a below. From the spectra we can see that, with the increase of preparation temperature, the intensities of peaks in position of 451 $cm^{-1}$, 967 $cm^{-1}$ and 1458 $cm^{-1}$ of the $C_{60}$ polymer crystal gradually decrease and finally disappear, indicating that the $C_{60}$ cages in polymer crystal are broken and the symmetry are severely reduced at higher temperatures. Fig. R1b below shows the Lorentz fittings of spectra for the carbons made at 540 °C and 575 °C, which have combined contribution of peaks ascribed to graphene, like the simulation for LOPC-550°C-5h in previous Fig. S7. For carbon prepared at 575 °C, the broad band centered at 1347 $cm^{-1}$ may be related to defects in graphene-like carbon, as indicated by the evolution of carbons from $C_{60}$ to graphite.

We have added the new Raman data in the revised Supplementary Information file.

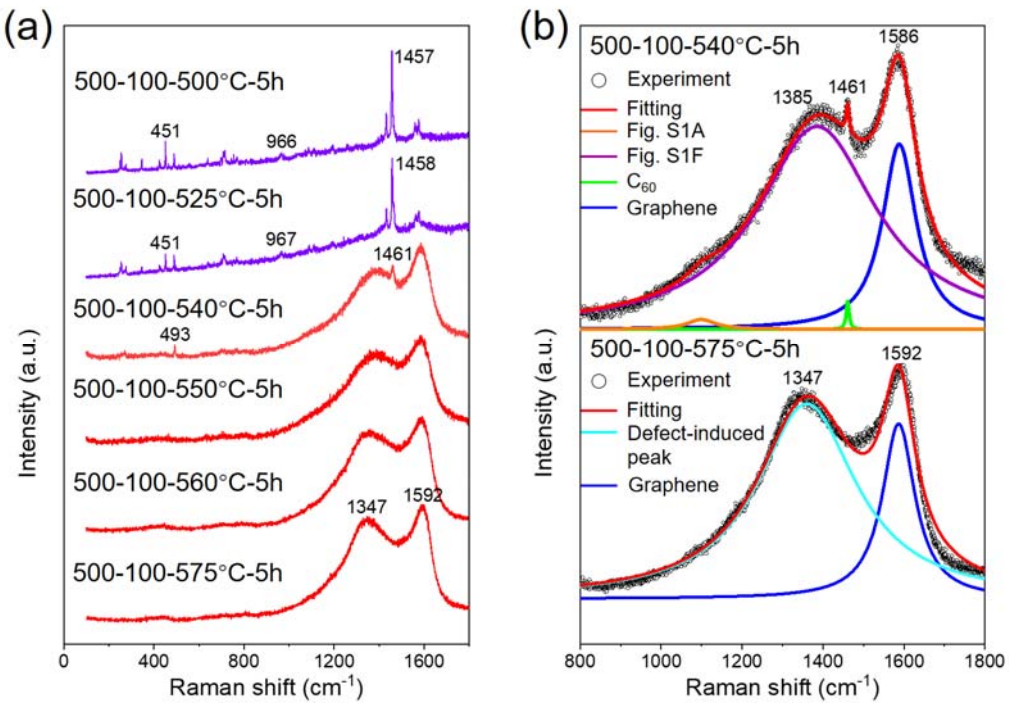


**Fig. R1.** (a) Raman spectra for carbons prepared by annealing 500 mg $C_{60}$ with 100 mg $\alpha$-$Li_3N$ for 5 h at different temperatures ranging from 500 to 575 °C (testing conditions: excitation wavelength of 532 nm, for the samples of 500-100-500°C-5h and 500-100-525°C-5h, laser power of 55 μW, integration time of 40 s or 20 s, accumulation number of 1; for the samples of 500-100-540°C-5h, 500-100-550°C-5h, 500-100-560°C-5h and 500-100-575°C-5h, laser power of 450 μW, integration time of 10 s, accumulation number of 6, 50x objective lens, grating of 1800 lines). (b) Lorentz fitting of Raman spectra of samples prepared at 540 °C and 575 °C with the Raman spectra of $C_{60}$, graphene, defect-induced peak and LOPC structures shown in **Fig. S1** A, **Fig. S1** F.